AIMS Mathematics

http://www.aimspress.com/journal/Math

AIMS Mathematics, 11(9): 30509–30544.
DOI:10.3934/math.20261209
Received: 01 July 2026
Revised: 03 September 2026
Accepted: 10 September 2026
Published: 20 September 2026

Research article

Fibonacci level m polynomial collocation algorithms for classical and time-fractional fifth-order Korteweg–de Vries equations

Mohamed Adel[1], **Ahmed Gamal Atta**[2], **Naher Mohammed A. Alsafri**[3], **Mohamed Abbas El-Naggar**[4,5] **and Waleed Mohamed Abd-Elhameed**[6,*]

[1] Department of Mathematics, Faculty of Science, Islamic University of Madinah, Medina, Saudi Arabia

[2] Department of Mathematics, Faculty of Education, Ain Shams University, Roxy 11341, Cairo, Egypt

[3] Department of Mathematics and Statistics, College of Science, University of Jeddah, Jeddah 23831, Saudi Arabia

[4] Department of General Subjects, University of Business and Technology, Jeddah 21361, Saudi Arabia

[5] Chemical Engineering Department, Faculty of Engineering, Alexandria University, Alexandria 21544, Egypt

[6] Department of Mathematics, Faculty of Science, Cairo University, Giza 12613, Egypt

* **Correspondence:** Email: waleed@cu.edu.eg.

Abstract: This work constructs and analyzes a spectral collocation procedure for the classical and time-fractional nonlinear fifth-order Korteweg–de Vries equations (NFOKDVEs). The approximation is built by using Fibonacci level m polynomials, a generalized form of the standard Fibonacci polynomial sequence. We derive several auxiliary results for this polynomial family, including an inversion relation, an integer-order differentiation formula, a fractional differentiation formula, and the corresponding operational matrices. These ingredients are then used to convert the nonlinear models under consideration into algebraic systems whose unknown coefficients are numerically determined using Newton's method. The performance of the resulting algorithms is tested through several examples. The reported errors, residuals, and comparisons with available methods show that the proposed polynomial basis produces accurate approximations with few expansion terms.

Keywords: Fibonacci numbers; Fibonacci polynomials; collocation method; operational matrices; nonlinear systems
Mathematics Subject Classification: 33C45, 35R11, 65M70

1. Introduction

Fractional differential equations (FDEs) have received significant attention in recent decades because they provide more realistic mathematical descriptions of many complex physical and engineering phenomena than their corresponding classical integer-order models. Such equations arise naturally in viscoelasticity, anomalous diffusion, fluid mechanics, heat transfer, control theory, biological systems, signal processing, and many other scientific disciplines; see [1–3]. Since exact closed-form solutions are unavailable for most nonlinear fractional models, the development of reliable numerical techniques has become an important topic in computational mathematics. Consequently, many numerical approaches have been introduced for solving FDEs. Related iterative and convergence techniques for differential systems can be found in [4, 5]. Among these approaches are the time-space collocation formulations [6], the hybrid Laplace–Adomian variational iteration procedure [7], Lyapunov-type methods [8], Laplace transform approaches [9], optimal control formulations [10], homotopy analysis schemes [11], collocation discrete least-squares meshless techniques [12], the L1-predictor–corrector strategy [13], and finite difference formulations [14].

Polynomial approximation methods have recently become powerful tools in numerical analysis for solving different classes of differential equations (DEs). Various orthogonal and non-orthogonal polynomial families have been incorporated into several approximation frameworks for solving ordinary, partial, integro-differential, and fractional DEs. In [15], Müntz–Legendre polynomial approximations were employed for solving fractional variational models. Chebyshev polynomial expansions were utilized in [16] for nonlinear Emden–Fowler delay DEs involving fractional derivatives. Pell coefficient polynomial approximations were investigated in [17] for solving hyperbolic partial DEs through a tau formulation. A Hermite polynomial least-squares method was considered in [18] for fractional Bagley–Torvik equations. In [19], a discrete Chebyshev polynomial approximations were utilized for two-dimensional fractional optimal control models involving Caputo–Hadamard derivatives. Gegenbauer polynomial approximations integrated with neural-network procedures were proposed in [20] for solving certain integral equations. Composite spectral approximations based on Legendre–Legendre rational polynomials were developed in [21] for Fokker–Planck equations on unbounded intervals. Generalized Legendre–Laguerre structures combined with fractional operators were studied in [22]. In addition, several recent studies focused on nonclassical polynomial families. Hosoya polynomial collocation procedures were developed in [23] for thermal transport models in trihybrid nanofluids. Chelyshkov polynomial approximations were considered in [24] for fractional tumor–immune interaction models. Generalized Bernoulli wavelet approximations were investigated in [25] for distributed-order FDEs. Shifted Vieta–Fibonacci polynomial formulations were proposed in [26] for nonlinear reaction–diffusion equations involving variable-order derivatives. Furthermore, shifted companion Morgan–Voyce polynomial approximations were employed in [27] to solve the time-fractional Kuramoto–Sivashinsky problem.

Spectral approaches are regarded as one of the most efficient and accurate numerical techniques for solving DEs. These methods approximate the unknown solution through truncated series expansions involving selected basis functions, which are usually chosen from orthogonal or non-orthogonal polynomial families. Unlike finite difference and finite element formulations that provide local approximations, spectral techniques produce global approximations over the entire computational interval. Another remarkable advantage of spectral methods is their capability of producing highly accurate numerical solutions while using only a relatively small number of basis functions; see [28, 29]. The most widely used spectral techniques are the collocation, tau, and Galerkin formulations. Among these approaches, the collocation method is particularly attractive because of its straightforward implementation and reduced computational complexity. For example, a B-spline collocation algorithm was introduced in [30] for a time-fractional Black–Scholes equation with jump-diffusion effects. A hybrid Daubechies wavelet collocation formulation was proposed in [31] for delayed fractional epidemic models. Chebyshev collocation approximations combined with overlapping-domain procedures were considered in [32] for eigenvalue problems. Dickson polynomial spectral approximations were utilized in [33] for several fractional physical models. On the other hand, tau and Galerkin methods generally require additional projection and integration procedures. Several recent tau formulations can be found in [34–36], while recent Galerkin formulations were investigated in [37–39].

The classical and fractional Korteweg–de Vries equations together with their generalized forms have attracted considerable attention because of their important applications in nonlinear wave propagation and fluid dynamics. Therefore, many analytical and numerical approaches have been developed for studying these equations. Analytical soliton solutions for the fractional generalized perturbed KdV equation were obtained in [40]. Generalized Jacobi–Galerkin operational matrices were employed in [41] for solving coupled time-fractional KdV systems. A pseudo-operational collocation procedure for variable-order KdV–Burgers–Kuramoto models was developed in [42]. The numerical dynamics of fractional nonlinear waves governed by fifth-order KdV and Kawahara equations were examined in [43]. In [44], a γ-robust numerical algorithm was introduced for the time-fractional nonlinear KdV equation. Coupled fractional modified KdV equations were solved in [45] using the Adomian decomposition procedure. Generalized exact solutions related to plasma-fluid models were discussed in [46]. Petrov–Galerkin approximations for coupled time-fractional KdV equations were considered in [47]. Exact solutions for coupled KdV and Boussinesq systems were derived in [48]. Soliton structures associated with seventh-order time-fractional KdV equations were investigated in [49]. Modified Exp-function approaches for traveling-wave solutions of modified KdV equations were discussed in [50]. In addition, non-central multi-point method-of-lines formulations for classical KdV equations were proposed in [51].

Operational matrix techniques have become effective computational tools for solving ordinary and partial DEs, especially those involving fractional operators. The main advantage of these formulations is that differential and integral operators are transformed into matrix representations, reducing the original equations into systems of algebraic equations. Considerable effort has recently been devoted to constructing operational matrices associated with different polynomial families. Vieta–Lucas polynomial operational matrices were developed in [52] for Caputo FDEs. Bernoulli wavelet operational matrices were utilized in [53] for nanofluid flow problems. Fractional Jacobi operational matrices were investigated in [54] for variable-order models. Operational matrix formulations for Poisson equations with nonlocal boundary conditions were considered in [55]. Fractional partial DEs were numerically treated in [56] through operational matrix procedures. Fibonacci wavelet frame operational matrices were applied in [57] for Arrhenius-controlled heat-transfer models. Shifted Pell polynomial formulations were proposed in [58] for Rosenau–Hyman and Gilson–Pickering equations. Shifted Dickson polynomial operational matrices were introduced in [59] for the time-fractional Huxley equation. Fibonacci coefficient polynomial approximations were also utilized in [60] to treat the time-fractional Kuramoto–Sivashinsky equation. Moreover, operational matrices related to fractional-order Lagrange polynomials were investigated in [61], while variable-order chemical process models were discussed in [62].

Motivated by the above investigations, we develop a highly accurate collocation framework for solving both the classical and time-fractional nonlinear fifth-order Korteweg–de Vries equations using Fibonacci level m polynomials, which generalize the standard Fibonacci polynomial family. Several new theoretical formulas associated with these polynomials are established, including inversion formulas together with explicit integer- and fractional-order derivative formulas and the corresponding operational matrices. These formulas are then utilized for constructing efficient spectral-collocation algorithms for the studied nonlinear models. The developed approach transforms the governing equations into systems of nonlinear algebraic equations that can be solved efficiently through Newton's iterative procedure. The obtained numerical results together with residual error analysis and comparisons with existing methods confirm the high accuracy and effectiveness of the proposed algorithms.

From a theoretical point of view, the novelty and advantages of the proposed Fibonacci level m polynomial basis over other polynomial sequences can be listed as follows:

- The parameter m generates a different polynomial sequence for every choice and hence a new approximation basis.
- The Fibonacci level m polynomials generalize the standard Fibonacci polynomials, which are recovered as a special case.
- The level parameter m provides additional flexibility in selecting the polynomial basis while retaining the same collocation framework.
- The inversion formula, integer- and fractional-order differentiation formulas, and the corresponding operational matrices can be conveniently derived from their explicit structure.

From a numerical point of view, the advantages of the proposed Fibonacci level m polynomial collocation algorithms can be listed as follows:

- High numerical accuracy can be achieved using a relatively small number of basis functions.
- The classical and time-fractional fifth-order KdV equations are reduced to finite systems of nonlinear algebraic equations that can be numerically treated using the operational matrix formulation.
- The same computational scheme can be successfully applied to both classical and time-fractional fifth-order KdV equations as well as other high-order KdV models.
- Numerical experiments reveal small residual errors, which verify the accuracy and reliability of the proposed approximations.
- The proposed algorithms are compared with existing numerical schemes, and their efficiency and accuracy are demonstrated.

The key objectives pursued in this article are as follows:

- Introducing level m polynomials that extend the celebrated Fibonacci polynomials.
- Deriving a new inversion formula for Fibonacci level m polynomials.
- Developing explicit formulas for the integer and fractional derivatives of Fibonacci level m polynomials.

- Constructing the corresponding operational matrices associated with Fibonacci level m polynomials.
- Developing highly accurate collocation algorithms for solving the classical and time-fractional nonlinear fifth-order Korteweg–de Vries equations.
- Transforming the studied nonlinear DEs into systems of algebraic equations through the proposed collocation procedures.
- Investigating the convergence and numerical accuracy of the developed algorithms.
- Demonstrating the effectiveness of the proposed methods through numerical examples, residual error analysis, and comparisons with available methods.

The remainder of this paper is organized as follows. Section 2 presents some preliminary definitions and related formulas. Section 3 derives new formulas associated with Fibonacci level m polynomials and their operational matrices. Section 4 develops a collocation approach for solving the classical nonlinear fifth-order Korteweg–de Vries equations. Section 5 extends the proposed approach to the time-fractional nonlinear fifth-order Korteweg–de Vries equations. Section 6 is devoted to the convergence and error analysis. Finally, Section 7 presents numerical experiments and comparative analysis, thereby validating the accuracy, robustness, and efficiency of the proposed approach.

2. Preliminaries and some related relations

This section collects some essential definitions. First, we recall the Caputo fractional derivative together with some of its fundamental properties. In addition, we introduce the Fibonacci level m polynomials and provide an overview of them.

2.1. Caputo fractional derivative

Definition 2.1. *The Caputo fractional derivative is recalled in the form [63]:*

$$D_z^{\zeta}\chi(z) = \frac{1}{\Gamma(s-\zeta)}\int_0^z (z-t)^{s-\zeta-1}\chi^{(s)}(t)\,dt, \quad \zeta > 0, \quad z > 0, \tag{2.1}$$

where

$$s-1 < \zeta \le s, \qquad s \in \mathbb{N}.$$

The following elementary relations are useful:

$$D_z^{\zeta} A = 0, \ (A \text{ is a constant}), \tag{2.2}$$

$$D_z^{\zeta} z^s = \begin{cases} 0, & \text{if } s \in \mathbb{N}_0 \quad \textit{and} \quad s < \lceil\zeta\rceil, \\ \frac{s!}{\Gamma(s+1-\zeta)}\, z^{s-\zeta}, & \text{if } s \in \mathbb{N}_0 \quad \textit{and} \quad s \ge \lceil\zeta\rceil, \end{cases} \tag{2.3}$$

where $\mathbb{N} = \{1, 2, \ldots\}$, $\mathbb{N}_0 = \{0, 1, 2, \ldots\}$, and $\lceil\zeta\rceil$ represents the ceiling function.

2.2. Fibonacci level m polynomials

The explicit power representation of the Fibonacci level m polynomials $\mathrm{F}_i^m(x)$ is defined as

$$\mathrm{F}_i^m(x) = \sum_{k=0}^{\lfloor \frac{i}{m} \rfloor} \binom{i-(m-1)k}{k} x^{i-km}, \tag{2.4}$$

that is, this expansion can be represented as

$$\mathrm{F}_i^m(x) = \sum_{k=0}^{i} \epsilon_{\frac{i-k}{m}} \binom{\frac{i+k(m-1)}{m}}{\frac{i-k}{m}} x^k, \tag{2.5}$$

where

$$\epsilon_i = \begin{cases} 1, & i \text{ integer}, \\ 0, & \text{otherwise}. \end{cases} \tag{2.6}$$

3. New identities for Fibonacci level m polynomials

This section develops several new expressions for the Fibonacci level m polynomials. These include an inversion formula and integer and fractional derivatives of these polynomials. These expressions will be the tools required for the numerical treatment presented later.

Lemma 3.1. *For each nonnegative integer L, the power x^L admits the following representation:*

$$x^L = \sum_{i=0}^{\lfloor L/m \rfloor} \frac{(-1)^i (1 + L - im)(L + 2 - i)_{i-1}}{i!} \mathrm{F}_{L-mi}^m(x). \tag{3.1}$$

Proof. Let

$$A_{L,m}(x) = \sum_{i=0}^{\lfloor L/m \rfloor} \frac{(-1)^i (1 + L - im)(L + 2 - i)_{i-1}}{i!} \mathrm{F}_{L-mi}^m(x). \tag{3.2}$$

Using (2.4), we expand $\mathrm{F}_{L-mi}^m(x)$ as

$$\mathrm{F}_{L-mi}^m(x) = \sum_{r=0}^{\lfloor (L-mi)/m \rfloor} \binom{L - mi - (m-1)r}{r} x^{L-mi-mr}, \tag{3.3}$$

and hence $A_{L,m}(x)$ takes the form

$$\begin{aligned} A_{L,m}(x) = \sum_{i=0}^{\lfloor L/m \rfloor} \sum_{r=0}^{\lfloor (L-mi)/m \rfloor} & \frac{(-1)^i (1 + L - im)(L + 2 - i)_{i-1}}{i!} \\ & \times \binom{L - mi - (m-1)r}{r} x^{L-mi-mr}. \end{aligned} \tag{3.4}$$

Setting $s = i + r$, relation (3.4) is transformed into

$$A_{L,m}(x) = \sum_{s=0}^{\lfloor L/m \rfloor} C_{L,s,m} \, x^{L-ms}, \tag{3.5}$$

where

$$C_{L,s,m} = \sum_{i=0}^{s} \frac{(-1)^i (1 + L - mi)(L + 2 - i)_{i-1}}{i!} \binom{L - (m-1)s - i}{s - i}. \tag{3.6}$$

After simplification, $C_{L,s,m}$ takes the following form:

$$C_{L,s,m} = (-1)^s \sum_{i=0}^{s} \binom{L+1}{i}\binom{ms-L-1}{s-i} + m(-1)^{s-1} \sum_{i=1}^{s} \binom{L}{i-1}\binom{ms-L-1}{s-i}. \tag{3.7}$$

We next evaluate the two sums in (3.7). Applying the Chu–Vandermonde identity

$$\sum_{i=0}^{s} \binom{\gamma}{i}\binom{\beta}{s-i} = \binom{\gamma+\beta}{s}, \tag{3.8}$$

with

$$\gamma = L+1, \qquad \beta = ms-L-1, \tag{3.9}$$

gives the following value for the first sum:

$$\sum_{i=0}^{s} \binom{L+1}{i}\binom{ms-L-1}{s-i} = \binom{ms}{s}. \tag{3.10}$$

For the second sum that appears in (3.7), set $j = i-1$ to get

$$\sum_{i=1}^{s} \binom{L}{i-1}\binom{ms-L-1}{s-i} = \sum_{j=0}^{s-1} \binom{L}{j}\binom{ms-L-1}{s-1-j}. \tag{3.11}$$

Applying the Chu–Vandermonde identity (3.8) again with $\gamma = L$ and $\beta = ms-L-1$ yields

$$\sum_{j=0}^{s-1} \binom{L}{j}\binom{ms-L-1}{s-1-j} = \binom{ms-1}{s-1}. \tag{3.12}$$

Combining (3.7), (3.10), and (3.12), we obtain

$$C_{L,s,m} = (-1)^s\binom{ms}{s} + m(-1)^{s-1}\binom{ms-1}{s-1}. \tag{3.13}$$

Using

$$\binom{ms}{s} = m\binom{ms-1}{s-1}, \tag{3.14}$$

we obtain from (3.13) that

$$C_{L,s,m} = 0, \qquad s \geq 1. \tag{3.15}$$

Also, for $s = 0$, we have

$$C_{L,0,m} = 1. \tag{3.16}$$

Thus, by (3.5), (3.15), and (3.16), we get

$$A_{L,m}(x) = x^L. \tag{3.17}$$

Combining (3.2) and (3.17), we obtain

$$x^L = \sum_{i=0}^{\lfloor L/m \rfloor} \frac{(-1)^i(1+L-im)(L+2-i)_{i-1}}{i!}\, \mathrm{F}^m_{L-mi}(x). \tag{3.18}$$

This establishes (3.1). □

Remark 3.1. *The inversion formula in Lemma 3.1 can be rewritten in another form as*

$$x^L = \sum_{i=0}^{L} H_{i,L}\, \mathrm{F}_i^m(x), \tag{3.19}$$

where

$$H_{i,L} = \frac{(i+1)(-1)^{\frac{L-i}{m}}\, \epsilon_{\frac{L-i}{m}} \left(L+2-\frac{L-i}{m}\right)_{\frac{L-i}{m}-1}}{\left(\frac{L-i}{m}\right)!}, \tag{3.20}$$

and ϵ_i is defined in (2.6).

Corollary 3.1. *Let $m \geq 2$, and let i, q be positive integers with $i \geq q$. Then the derivative of $\mathrm{F}_i^m(x)$ can be expressed in the following forward form:*

$$D^q \mathrm{F}_i^m(x) = \sum_{r=0}^{i-q} \lambda_{i,r,q}^{(m)}\, \mathrm{F}_r^m(x), \tag{3.21}$$

where

$$\begin{aligned} \lambda_{i,r,q}^{(m)} &= \epsilon_{\frac{i-q-r}{m}} \frac{(-1)^{\frac{i-q-r}{m}}(1+r)i!}{\left(\frac{i-q-r}{m}\right)! \left(i-q-\frac{i-q-r}{m}+1\right)!} \\ &\times {}_mF_{m-1}\left(\left.\begin{matrix} -\frac{i-q-r}{m},\ \Delta\left(m-1;\ q+\frac{i-q-r}{m}-i-1\right) \\ \Delta\left(m-1;\ -i\right) \end{matrix}\right| 1\right). \end{aligned} \tag{3.22}$$

Here,

$$\Delta(M;a) = \left\{\frac{a}{M}, \frac{a+1}{M}, \dots, \frac{a+M-1}{M}\right\}, \tag{3.23}$$

and ϵ_i is as defined in (2.6).

Proof. Differentiating the series representation (2.4) q times gives

$$\frac{d^q \mathrm{F}_i^m(x)}{dx^q} = \sum_{t=0}^{\left\lfloor \frac{i-q}{m} \right\rfloor} \binom{i-(m-1)t}{t} \frac{(i-mt)!}{(i-q-mt)!} x^{i-q-mt}. \tag{3.24}$$

Applying the inversion relation (3.1) with $L = i-q-mt$, we obtain

$$\begin{aligned} x^{i-q-mt} = \sum_{s=0}^{\left\lfloor \frac{i-q-mt}{m} \right\rfloor} & \frac{(-1)^s(1+i-q-mt-ms)(2-s+i-q-mt)_{s-1}}{s!} \\ & \times \mathrm{F}_{i-q-mt-ms}^m(x). \end{aligned} \tag{3.25}$$

Substituting (3.25) into (3.24), we get

$$\begin{aligned}\frac{d^q \mathrm{F}_i^m(x)}{dx^q} = &\sum_{t=0}^{\left\lfloor \frac{i-q}{m} \right\rfloor} \binom{i+t-mt}{t} \frac{(i-mt)!}{(i-q-mt)!}\\ &\times \sum_{s=0}^{\left\lfloor \frac{i-q-mt}{m} \right\rfloor} \frac{(-1)^s (1+i-q-mt-ms)(2-s+i-q-mt)_{s-1}}{s!}\\ &\times \mathrm{F}_{i-q-mt-ms}^m(x).\end{aligned} \tag{3.26}$$

With the index transformation

$$L = t + s, \qquad s = L - t, \tag{3.27}$$

the summation limits become

$$0 \le L \le \left\lfloor \frac{i-q}{m} \right\rfloor, \qquad 0 \le t \le L. \tag{3.28}$$

Hence, (3.26) can be rewritten as

$$\begin{aligned}\frac{d^q \mathrm{F}_i^m(x)}{dx^q} = \sum_{L=0}^{\left\lfloor \frac{i-q}{m} \right\rfloor} \Bigg[\sum_{t=0}^{L} &\frac{(-1)^{L-t}(1+i-q-mL)\binom{1+i-q-mt}{L-t}}{(1+i-q-mt)!}\\ &\times \binom{i+t-mt}{t} (i-mt)! \Bigg] \mathrm{F}_{i-q-mL}^m(x).\end{aligned} \tag{3.29}$$

The inner finite sum in (3.29) can be expressed in the hypergeometric form

$$\begin{aligned}\mathcal{A}_{i,L,q}^{(m)} = &\frac{(-1)^L (1+i-q-mL) i!}{L!\,(i-q-L+1)!}\\ &\times {}_mF_{m-1}\left(\left. \begin{matrix} -L,\ \Delta(m-1;\ q+L-i-1) \\ \\ \Delta(m-1;\ -i) \end{matrix} \right| 1 \right).\end{aligned} \tag{3.30}$$

Therefore, we obtain the backward representation

$$D^q \mathrm{F}_i^m(x) = \sum_{L=0}^{\left\lfloor \frac{i-q}{m} \right\rfloor} \mathcal{A}_{i,L,q}^{(m)}\, \mathrm{F}_{i-q-mL}^m(x). \tag{3.31}$$

Equivalently, the backward representation (3.31) can be written in the forward form (3.21). This completes the proof. □

Remark 3.2. *As a consequence of Corollary 3.1, considering the vector*

$$\mathbf{F}_\sigma^m = [\mathrm{F}_0^m(\sigma), \mathrm{F}_1^m(\sigma), \ldots, \mathrm{F}_{\mathcal{L}}^m(\sigma)]^T, \tag{3.32}$$

the derivatives of order p of the vector $\mathbf{F}_\sigma^m$ may be expressed in the following matrix form:

$$\frac{d^p\, \mathbf{F}_\sigma^m}{d\,\sigma^p} = \boldsymbol{A}^p\, \mathbf{F}_\sigma^m, \tag{3.33}$$

where $\boldsymbol{A} = (\mathcal{A}_{i,L,q}^{(m)})$ is the operational matrix of derivatives of order $(\mathcal{L}+1)^2$.

Theorem 3.1. *For $\beta \in (0,1)$, the values of the fractional derivative of $\mathrm{F}_j^m(t)$ can be represented at a set of distinct collocation points $\{t_i\}_{i=1}^{\mathcal{L}+1} \subset [0,1]$ by*

$$D_t^\beta \mathrm{F}_j^m(t_i) = \sum_{n=0}^{\mathcal{L}} \mu_{j,n}^\beta \, \mathrm{F}_n^m(t_i), \tag{3.34}$$

where

$$\mu_{j,n}^\beta = \sum_{i=1}^{\mathcal{L}+1} \zeta_j(t_i) \left(\phi^{-1}\right)_{i,n+1}, \tag{3.35}$$

$$\zeta_j(t_i) = \sum_{k=0}^{j} \binom{\frac{j+k(m-1)}{m}}{\frac{j-k}{m}} \frac{\epsilon_{\frac{j-k}{m}} \, k!}{\Gamma(k-\beta+1)} t_i^{k-\beta}, \tag{3.36}$$

and $\left(\phi^{-1}\right)_{i,r+1}$ are the elements resulting from the inverse of the matrix $\mathbf{\Phi} = (\mathrm{F}_r^m(t_i))_{(\mathcal{L}+1)\times(\mathcal{L}+1)}$.

Proof. Using Definition (2.3) together with formula (2.5) yields $D_t^\beta \, \mathrm{F}_j^m(t)$ as

$$D_t^\beta \, \mathrm{F}_j^m(t) = \sum_{k=0}^{j} \binom{\frac{j+k(m-1)}{m}}{\frac{j-k}{m}} \frac{\epsilon_{\frac{j-k}{m}} \, k!}{\Gamma(k-\beta+1)} t^{k-\beta}. \tag{3.37}$$

Next, we approximate $t^{k-\beta}$ in a finite-dimensional discrete space using a set of $\mathcal{L}+1$ distinct collocation points

$$t_i \in [0,1], \qquad i = 1, 2, \ldots, \mathcal{L}+1.$$

Thus, Eq (3.37) can be written as

$$\zeta_j(t_i) = D_t^\beta \, \mathrm{F}_j^m(t_i) = \sum_{k=0}^{j} \binom{\frac{j+k(m-1)}{m}}{\frac{j-k}{m}} \frac{\epsilon_{\frac{j-k}{m}} \, k!}{\Gamma(k-\beta+1)} t_i^{k-\beta}. \tag{3.38}$$

Assume now that $D_t^\beta \, \mathrm{F}_j^m(t_i)$ is expanded in the basis $\mathrm{F}_r^m(t_i)$ as

$$D_t^\beta \mathrm{F}_j^m(t_i) = \sum_{r=0}^{\mathcal{L}} \mu_{j,r}^\beta \, \mathrm{F}_r^m(t_i). \tag{3.39}$$

From Eqs (3.38) and (3.39), we can write

$$\zeta_j(t_i) = \sum_{r=0}^{\mathcal{L}} \mu_{j,r}^\beta \, \mathrm{F}_r^m(t_i). \tag{3.40}$$

To determine $\mu_{j,n}^\beta$, we let $\mathbf{\Phi} = (\phi_{r+1,i} = \mathrm{F}_r^m(t_i))_{(\mathcal{L}+1)\times(\mathcal{L}+1)}$ denote the collocation matrix of the basis.

Because the polynomials $\{\mathrm{F}_n^m(t)\}_{n=0}^{\mathcal{L}}$ are linearly independent and the nodes t_i are distinct, the interpolation matrix $\mathbf{\Phi}$ is nonsingular and therefore has a unique inverse, $\mathbf{\Phi}^{-1}$, which satisfies

$$\sum_{i=1}^{\mathcal{L}+1} \phi_{n+1,i} \left(\phi^{-1}\right)_{i,r+1} = \delta_{n,r}, \tag{3.41}$$

where $\delta_{n,r}$ is the Kronecker delta function.

Multiplying both sides of Eq (3.40) by the elements of the inverse interpolation matrix $\left(\phi^{-1}\right)_{i,n+1}$ and taking $\sum_{i=1}^{\mathcal{L}+1}$, we get

$$\sum_{i=1}^{\mathcal{L}+1} \zeta_j(t_i) \left(\phi^{-1}\right)_{i,n+1} = \sum_{r=0}^{\mathcal{L}} \mu_{j,r}^{\beta} \left[\sum_{i=1}^{\mathcal{L}+1} \phi_{r+1,\,i} \left(\phi^{-1}\right)_{i,\,n+1}\right]. \tag{3.42}$$

Finally, employing the property defined in (3.41), we get

$$\mu_{j,n}^{\beta} = \sum_{i=1}^{\mathcal{L}+1} \zeta_j(t_i) \left(\phi^{-1}\right)_{i,n+1}. \tag{3.43}$$

□

Remark 3.3. *As a consequence of Theorem 3.1, the fractional derivative of the vector* $\mathbf{F}_t^{\,m}$ *can be represented in matrix form:*

$$D_t^{\beta}\, \mathbf{F}_t^{\,m} = \boldsymbol{\mu}^{\beta}\, \mathbf{F}_t^{\,m}, \tag{3.44}$$

where $\boldsymbol{\mu}^{\beta} = \boldsymbol{D}^{\beta}\, \boldsymbol{\Phi}^{-1}$ is the operational matrix of derivatives of order $(\mathcal{L}+1)^2$.

$$\boldsymbol{D}^{\beta} = \begin{bmatrix} 0 & 0 & \cdots & 0 \\ \zeta_1(t_1) & \zeta_1(t_2) & \cdots & \zeta_1(t_{\mathcal{L}+1}) \\ \vdots & \vdots & \ddots & \vdots \\ \zeta_{\mathcal{L}}(t_1) & \zeta_{\mathcal{L}}(t_2) & \cdots & \zeta_{\mathcal{L}}(t_{\mathcal{L}+1}) \end{bmatrix},$$

$$\boldsymbol{\Phi} = \begin{bmatrix} \mathrm{F}_0^m(t_1) & \mathrm{F}_0^m(t_2) & \cdots & \mathrm{F}_0^m(t_{\mathcal{L}+1}) \\ \mathrm{F}_1^m(t_1) & \mathrm{F}_1^m(t_2) & \cdots & \mathrm{F}_1^m(t_{\mathcal{L}+1}) \\ \vdots & \vdots & \ddots & \vdots \\ \mathrm{F}_{\mathcal{L}}^m(t_1) & \mathrm{F}_{\mathcal{L}}^m(t_2) & \cdots & \mathrm{F}_{\mathcal{L}}^m(t_{\mathcal{L}+1}) \end{bmatrix}.$$

4. Collocation formulation for the classical NFOKDVEs

In this section, a Fibonacci level m polynomial collocation algorithm is developed for solving the classical nonlinear fifth-order KdV equations. The proposed formulation transforms the governing nonlinear equation into a nonlinear algebraic system using operational derivative matrices.

Consider the NFOKDVEs [64, 65]:

$$\begin{aligned} &\frac{\partial\, \mathcal{Z}(\sigma,t)}{\partial\, t} + a\, \mathcal{Z}(\sigma,t)^2 \left(\frac{\partial\, \mathcal{Z}(\sigma,t)}{\partial\, \sigma}\right) + b \left(\frac{\partial\, \mathcal{Z}(\sigma,t)}{\partial\, \sigma}\right)\left(\frac{\partial^2\, \mathcal{Z}(\sigma,t)}{\partial\, \sigma^2}\right) \\ &+ d\, \mathcal{Z}(\sigma,t) \left(\frac{\partial^3\, \mathcal{Z}(\sigma,t)}{\partial\, \sigma^3}\right) + \frac{\partial^5\, \mathcal{Z}(\sigma,t)}{\partial\, \sigma^5} = 0, \quad 0 \le \sigma, t \le 1, \end{aligned} \tag{4.1}$$

subject to the initial and boundary data

$$\mathcal{Z}(\sigma,0) = f(\sigma), \tag{4.2}$$

$$\mathcal{Z}(0,t) = h_0(t), \quad \mathcal{Z}(1,t) = h_1(t), \tag{4.3}$$

$$\frac{\partial\,\mathcal{Z}(0,t)}{\partial\,\sigma} = h_2(t), \quad \frac{\partial\,\mathcal{Z}(1,t)}{\partial\,\sigma} = h_3(t), \quad \frac{\partial^2\,\mathcal{Z}(0,t)}{\partial\,\sigma^2} = h_4(t), \tag{4.4}$$

and a, b, and d are prescribed constants.

Let us introduce the approximation space

$$\mathcal{X}^{\mathcal{L}} = \operatorname{span}\{\mathrm{F}_i^m(\sigma)\,\mathrm{F}_j^m(t) : 0 \le i, j \le \mathcal{L}\}. \tag{4.5}$$

Accordingly, any function $\mathcal{Z}_{\mathcal{L}}(\sigma,t) \in \mathcal{X}^{\mathcal{L}}$ is approximated by

$$\mathcal{Z}_{\mathcal{L}}(\sigma,t) = \sum_{i=0}^{\mathcal{L}}\sum_{j=0}^{\mathcal{L}} \hat{\mathcal{Z}}_{ij}\,\mathrm{F}_i^m(\sigma)\,\mathrm{F}_j^m(t) = \mathbf{F}_\sigma^{mT}\,\hat{\mathcal{Z}}\,\mathbf{F}_t^m, \tag{4.6}$$

where $\mathbf{F}_\sigma^m$ is given in (3.32), and $\hat{\mathcal{Z}} = (\hat{\mathcal{Z}}_{ij})_{0\le i,j\le\mathcal{L}}$ denotes the unknown coefficient matrix, whose order is $(\mathcal{L}+1)^2$.
The residual $\mathcal{R}^1_{\mathcal{L}}(\sigma,t)$ of Eq (4.1) is given by

$$\begin{aligned}\mathcal{R}^1_{\mathcal{L}}(\sigma,t) = {}& \frac{\partial\,\mathcal{Z}_{\mathcal{L}}(\sigma,t)}{\partial\,t} + a\,\mathcal{Z}_{\mathcal{L}}(\sigma,t)^2\left(\frac{\partial\,\mathcal{Z}_{\mathcal{L}}(\sigma,t)}{\partial\,\sigma}\right) + b\left(\frac{\partial\,\mathcal{Z}_{\mathcal{L}}(\sigma,t)}{\partial\,\sigma}\right)\left(\frac{\partial^2\,\mathcal{Z}_{\mathcal{L}}(\sigma,t)}{\partial\,\sigma^2}\right)\\ &+ d\,\mathcal{Z}_{\mathcal{L}}(\sigma,t)\left(\frac{\partial^3\,\mathcal{Z}_{\mathcal{L}}(\sigma,t)}{\partial\,\sigma^3}\right) + \frac{\partial^5\,\mathcal{Z}_{\mathcal{L}}(\sigma,t)}{\partial\,\sigma^5}.\end{aligned} \tag{4.7}$$

Using Remark 3.2 together with the expansion (4.6), the required derivative and nonlinear terms, $\frac{\partial\mathcal{Z}_{\mathcal{L}}(\sigma,t)}{\partial t}$, $\mathcal{Z}_{\mathcal{L}}(\sigma,t)^2\left(\frac{\partial\mathcal{Z}_{\mathcal{L}}(\sigma,t)}{\partial\sigma}\right)$, $\left(\frac{\partial^2\mathcal{Z}_{\mathcal{L}}(\sigma,t)}{\partial\sigma^2}\right)$, $\mathcal{Z}_{\mathcal{L}}(\sigma,t)\left(\frac{\partial^3\mathcal{Z}_{\mathcal{L}}(\sigma,t)}{\partial\sigma^3}\right)$, and $\frac{\partial^5\mathcal{Z}_{\mathcal{L}}(\sigma,t)}{\partial\sigma^5}$, are obtained:

$$\frac{\partial\mathcal{Z}_{\mathcal{L}}(\sigma,t)}{\partial t} = \mathbf{F}_\sigma^{mT}\,\hat{\mathcal{Z}}\,(\boldsymbol{A}^1\,\mathbf{F}_t^m), \tag{4.8}$$

$$\mathcal{Z}_{\mathcal{L}}(\sigma,t)^2\left(\frac{\partial\mathcal{Z}_{\mathcal{L}}(\sigma,t)}{\partial\sigma}\right) = [\mathbf{F}_\sigma^{mT}\,\hat{\mathcal{Z}}\,\mathbf{F}_t^m]^2\,[(\boldsymbol{A}^1\,\mathbf{F}_\sigma^m)^T\,\hat{\mathcal{Z}}\,\mathbf{F}_t^m], \tag{4.9}$$

$$\left(\frac{\partial\mathcal{Z}_{\mathcal{L}}(\sigma,t)}{\partial\sigma}\right)\left(\frac{\partial^2\mathcal{Z}_{\mathcal{L}}(\sigma,t)}{\partial\sigma^2}\right) = [(\boldsymbol{A}^1\,\mathbf{F}_\sigma^m)^T\,\hat{\mathcal{Z}}\,\mathbf{F}_t^m]\,[(\boldsymbol{A}^2\,\mathbf{F}_\sigma^m)^T\,\hat{\mathcal{Z}}\,\mathbf{F}_t^m], \tag{4.10}$$

$$\mathcal{Z}_{\mathcal{L}}(\sigma,t)\left(\frac{\partial^3\mathcal{Z}_{\mathcal{L}}(\sigma,t)}{\partial\sigma^3}\right) = [\mathbf{F}_\sigma^{mT}\,\hat{\mathcal{Z}}\,\mathbf{F}_t^m]\,[(\boldsymbol{A}^3\,\mathbf{F}_\sigma^m)^T\,\hat{\mathcal{Z}}\,\mathbf{F}_t^m], \tag{4.11}$$

$$\frac{\partial^5\mathcal{Z}_{\mathcal{L}}(\sigma,t)}{\partial\sigma^5} = (\boldsymbol{A}^5\,\mathbf{F}_\sigma^m)^T\,\hat{\mathcal{Z}}\,\mathbf{F}_t^m. \tag{4.12}$$

Using the relations (4.8)–(4.12), the residual $\mathcal{R}^1_{\mathcal{L}}(\sigma,t)$ is obtained in the form

$$\begin{aligned}\mathcal{R}^1_{\mathcal{L}}(\sigma,t) = {}& \mathbf{F}_\sigma^{mT}\hat{\mathcal{Z}}(\boldsymbol{A}^1\mathbf{F}_t^m) + a\,[\mathbf{F}_\sigma^{mT}\hat{\mathcal{Z}}\mathbf{F}_t^m]^2[(\boldsymbol{A}^1\mathbf{F}_\sigma^m)^T\hat{\mathcal{Z}}\mathbf{F}_t^m]\\ &+ b\,[(\boldsymbol{A}^1\mathbf{F}_\sigma^m)^T\hat{\mathcal{Z}}\mathbf{F}_t^m][(\boldsymbol{A}^2\mathbf{F}_\sigma^m)^T\hat{\mathcal{Z}}\mathbf{F}_t^m]\\ &+ d\,[\mathbf{F}_\sigma^{mT}\hat{\mathcal{Z}}\mathbf{F}_t^m][(\boldsymbol{A}^3\mathbf{F}_\sigma^m)^T\hat{\mathcal{Z}}\mathbf{F}_t^m] + (\boldsymbol{A}^5\mathbf{F}_\sigma^m)^T\hat{\mathcal{Z}}\mathbf{F}_t^m.\end{aligned} \tag{4.13}$$

To determine the expansion coefficients $\hat{\mathcal{Z}}_{ij}$, the residual $\mathcal{R}^1_{\mathcal{L}}(\sigma, t)$ is required to vanish at the collocation points $(\sigma_r, t_s) = \left(\frac{r}{\mathcal{L}+1}, \frac{s}{\mathcal{L}+1}\right)$ as follows:

$$\mathcal{R}^1_{\mathcal{L}}(\sigma_r, t_s) = 0, \quad 1 \le r \le \mathcal{L} - 4, \quad 1 \le s \le \mathcal{L}. \tag{4.14}$$

The constraints in (4.2)–(4.4) give the following algebraic equations:

$$\mathbf{F}^{m\,T}_{\sigma_r} \, \hat{\mathcal{Z}} \, \mathbf{F}^m_0 = f(\sigma_r), \quad 1 \le r \le \mathcal{L} + 1, \tag{4.15}$$
$$\mathbf{F}^{mT}_0 \, \hat{\mathcal{Z}} \, \mathbf{F}^m_{t_s} = h_0\,(t_s), \quad 1 \le s \le \mathcal{L}, \tag{4.16}$$
$$\mathbf{F}^{mT}_1 \, \hat{\mathcal{Z}} \, \mathbf{F}^m_{t_s} = h_1\,(t_s), \quad 1 \le s \le \mathcal{L}, \tag{4.17}$$
$$(\boldsymbol{A}^1 \, \mathbf{F}^m_0)^T \, \hat{\mathcal{Z}} \, \mathbf{F}^m_{t_s} = h_2\,(t_s), \quad 1 \le s \le \mathcal{L}, \tag{4.18}$$
$$(\boldsymbol{A}^1 \, \mathbf{F}^m_1)^T \, \hat{\mathcal{Z}} \, \mathbf{F}^m_{t_s} = h_3\,(t_s), \quad 1 \le s \le \mathcal{L}, \tag{4.19}$$
$$(\boldsymbol{A}^2 \, \mathbf{F}^m_0)^T \, \hat{\mathcal{Z}} \, \mathbf{F}^m_{t_s} = h_4\,(t_s), \quad 1 \le s \le \mathcal{L}. \tag{4.20}$$

The nonlinear algebraic system of order $(\mathcal{L} + 1)^2$, generated from Eqs (4.15)–(4.20) together with Eq (4.14), is solved using Newton's iterative method. Consequently, the numerical solution expressed in (4.6) can be determined.

5. Collocation formulation for the time-fractional NFOKDVEs

This section analyzes a Fibonacci level m polynomial collocation formulation for treating the time-fractional nonlinear fifth-order KdV equations. The fractional operational matrix of derivatives of the basis functions converts the problem governed by its conditions into a nonlinear algebraic system that can be solved using Newton's iterative procedure.

Consider the time-fractional NFOKDVEs [64]:

$$\begin{aligned}
&\frac{\partial^\beta \mathcal{Z}(\sigma, t)}{\partial t^\beta} + a\,\mathcal{Z}(\sigma, t)^2 \left(\frac{\partial \mathcal{Z}(\sigma, t)}{\partial \sigma}\right) + b \left(\frac{\partial \mathcal{Z}(\sigma, t)}{\partial \sigma}\right)\left(\frac{\partial^2 \mathcal{Z}(\sigma, t)}{\partial \sigma^2}\right) \\
&+ d\,\mathcal{Z}(\sigma, t) \left(\frac{\partial^3 \mathcal{Z}(\sigma, t)}{\partial \sigma^3}\right) + \frac{\partial^5 \mathcal{Z}(\sigma, t)}{\partial \sigma^5} = 0, \quad 0 < \beta < 1, \quad 0 \le \sigma, t \le 1,
\end{aligned} \tag{5.1}$$

with the initial and boundary conditions in (4.2)–(4.4).

From Remark 3.3 together with the expansion (4.6), the following matrix representation for the term $\frac{\partial^\beta \mathcal{Z}(\sigma,t)}{\partial t^\beta}$ is obtained:

$$\frac{\partial^\beta \mathcal{Z}(\sigma, t)}{\partial t^\beta} = \mathbf{F}^{mT}_\sigma \, \hat{\mathcal{Z}} \, (\boldsymbol{\mu}^\beta \, \mathbf{F}_t{}^m). \tag{5.2}$$

Using the relations (4.9)–(4.12) together with (5.2), the residual $\mathcal{R}^2_{\mathcal{L}}(\sigma, t)$ is obtained in the form:

$$\begin{aligned}
\mathcal{R}^2_{\mathcal{L}}(\sigma, t) = {} & \mathbf{F}^{mT}_\sigma \hat{\mathcal{Z}} \left(\boldsymbol{\mu}^\beta \mathbf{F}^m_t\right) + a \left[\mathbf{F}^{mT}_\sigma \hat{\mathcal{Z}} \mathbf{F}^m_t\right]^2 \left[(\boldsymbol{A}^1 \mathbf{F}^m_\sigma)^T \hat{\mathcal{Z}} \mathbf{F}^m_t\right] \\
& + b \left[(\boldsymbol{A}^1 \mathbf{F}^m_\sigma)^T \hat{\mathcal{Z}} \mathbf{F}^m_t\right] \left[(\boldsymbol{A}^2 \mathbf{F}^m_\sigma)^T \hat{\mathcal{Z}} \mathbf{F}^m_t\right] \\
& + d \left[\mathbf{F}^{mT}_\sigma \hat{\mathcal{Z}} \mathbf{F}^m_t\right] \left[(\boldsymbol{A}^3 \mathbf{F}^m_\sigma)^T \hat{\mathcal{Z}} \mathbf{F}^m_t\right] + (\boldsymbol{A}^5 \mathbf{F}^m_\sigma)^T \hat{\mathcal{Z}} \mathbf{F}^m_t.
\end{aligned} \tag{5.3}$$

The collocation procedure produces $(\mathcal{L}-4)\times\mathcal{L}$ algebraic equations from the relation

$$\mathcal{R}^2_{\mathcal{L}}(\sigma_r, t_s) = 0, \quad 1 \le r \le \mathcal{L}-4, \quad 1 \le s \le \mathcal{L}, \tag{5.4}$$

together with $(6\,\mathcal{L}+1)$ equations given in (4.15)–(4.20), where $(\sigma_r, t_s) = \left(\frac{r}{\mathcal{L}+1}, \frac{s}{\mathcal{L}+1}\right)$. Newton's iterative procedure is then applied to compute the unknown values $\hat{\mathcal{Z}}_{ij}$.

6. Convergence and error estimates

This section investigates the convergence of the Fibonacci level m polynomial expansions that are used to ensure the proposed approximate summation. We first establish a bound for the Fibonacci level m polynomials and derive estimates for the corresponding expansion coefficients. These estimations are pivotal in proving the absolute convergence of the series representations and obtaining explicit truncation error bounds for the finite approximation $\mathcal{Z}_{\mathcal{L}}(\sigma, t)$.

Lemma 6.1. *The following estimate holds for* $\mathrm{F}^m_i(\sigma)$*:*

$$|\mathrm{F}^m_i(\sigma)| < 2^{i+m}, \quad \sigma \in [0,1]. \tag{6.1}$$

Proof. Using (2.4), we get

$$\left|\mathrm{F}^m_i(\sigma)\right| \le \sum_{k=0}^{\lfloor \frac{i}{m} \rfloor} \binom{i-(m-1)k}{k}. \tag{6.2}$$

Based on the Pascal triangle estimate, we can write

$$\binom{i-(m-1)k}{k} < 2^{i-k(m-1)}, \tag{6.3}$$

and therefore, we get

$$\begin{aligned} \left|\mathrm{F}^m_i(\sigma)\right| &\le 2^i \sum_{k=0}^{\lfloor \frac{i}{m} \rfloor} 2^{-k\,(m-1)} \\ &= \frac{2^i \left(2^m - 2^{1-(m-1)\lfloor \frac{i}{m} \rfloor}\right)}{2^m - 2} \\ &< 2^{i+m}. \end{aligned} \tag{6.4}$$

This ends the proof. □

Lemma 6.2. *Suppose that* $g(\sigma)$ *is infinitely differentiable at* $\sigma = 0$*. We can write*

$$g(\sigma) = \sum_{n=0}^{\infty} \sum_{s=n}^{\infty} \frac{g^{(s)}(0)\, H_{n,s}}{s!}\, \mathrm{F}^m_n(\sigma), \tag{6.5}$$

where $H_{n,s}$ is defined in Eq (3.20).

Proof. The proof of this lemma is similar to the proof of Lemma 2 in [66]. □

Theorem 6.1. *If $g(\sigma)$ is defined on $[0,1]$, and $|g^{(i)}(0)| \leq \lambda^i$, $i > 0$, where $\lambda > 0$, and $g(\sigma) = \sum_{i=0}^{\infty} a_i \, \mathrm{F}_i^m(\sigma)$, then we get*

$$|a_i| \leq \frac{e^{2\lambda} \, 4^{-m} \, (2\lambda)^i}{i!}. \tag{6.6}$$

It is also worth noting that the series converges absolutely.

Proof. Lemma 6.2 implies that

$$|a_i| = \left| \sum_{s=i}^{\infty} \frac{g^{(s)}(0) \, H_{i,s}}{s!} \right| \leq \sum_{s=i}^{\infty} \frac{\left|g^{(s)}(0)\right| \left|H_{i,s}\right|}{s!}. \tag{6.7}$$

Equation (3.20) implies that, for $m \geq 1$ and $i \leq s < \infty$,

$$\left|H_{i,s}\right| < 2^{s-2m}. \tag{6.8}$$

The application of the assumption $|g^{(i)}(0)| \leq \lambda^i, i > 0$ enables us to write

$$|a_i| \leq \sum_{s=i}^{\infty} \frac{2^{s-2m} \lambda^s}{s!} = \frac{e^{2\lambda} 4^{-m} (\Gamma(i) - \Gamma(i, 2\lambda))}{\Gamma(i)}, \tag{6.9}$$

where $\Gamma(i, 2\lambda)$ represents the incomplete gamma function.

Based on the following inequality:

$$\frac{e^{2\lambda} 4^{-m} (\Gamma(i) - \Gamma(i, 2\lambda))}{\Gamma(i)} < \frac{e^{2\lambda} 4^{-m} (2\lambda)^i}{i!}, \quad \forall \, i > 0, \tag{6.10}$$

inequality (6.9) implies

$$|a_i| < \frac{e^{2\lambda} 4^{-m} (2\lambda)^i}{i!}. \tag{6.11}$$

The second statement of the theorem is an immediate consequence of inequalities (6.1) and (6.6). In fact,

$$\begin{aligned} \left| \sum_{i=0}^{\infty} a_i \, \mathrm{F}_i^m(\sigma) \right| &\leq \sum_{i=0}^{\infty} |a_i| \left| \mathrm{F}_i^m(\sigma) \right| \\ &\leq e^{6\lambda} 2^{-m}. \end{aligned} \tag{6.12}$$

Hence the series converges absolutely. □

Theorem 6.2. *Let $\mathcal{Z}(\sigma, t) = f_1(\sigma) \, f_2(t) = \sum_{i=0}^{\infty} \sum_{j=0}^{\infty} \hat{\mathcal{Z}}_{ij} \, \mathrm{F}_i^m(\sigma) \, \mathrm{F}_j^m(t)$, with $|f_1^{(i)}(0)| \leq \lambda_1^i$, $i > 0$ and $|f_2^{(j)}(0)| \leq \lambda_2^j$, $j > 0$, where λ_1 and λ_2 are positive constants. We get*

$$|\hat{\mathcal{Z}}_{ij}| < \frac{e^{2\lambda_1 + 2\lambda_2} \, 4^{-2m} \, 2^{i+j} \, \lambda_1^i \, \lambda_2^j}{i! \, j!}. \tag{6.13}$$

Furthermore, the series is absolutely convergent.

Proof. Based on Lemma 6.2 along with the stated assumption $\mathcal{Z}(\sigma, t) = f_1(\sigma)\, f_2(t)$, we get

$$\hat{\mathcal{Z}}_{ij} = \sum_{s=i}^{\infty} \sum_{q=j}^{\infty} \frac{f_1^{(s)}(0)\, f_2^{(q)}(0)\, H_{j,q}\, H_{i,s}}{s!\, q!}. \tag{6.14}$$

Based on the assumptions $|f_1^{(i)}(0)| \leq \lambda_1^i$ and $|f_2^{(i)}(0)| \leq \lambda_2^i$, we can write

$$|\hat{\mathcal{Z}}_{ij}| \leq \sum_{s=i}^{\infty} \frac{\lambda_1^s\, H_{i,s}}{s!} \times \sum_{q=j}^{\infty} \frac{\lambda_2^q\, H_{j,q}}{q!}. \tag{6.15}$$

Proceeding analogously to the argument presented in Theorem 6.1, we obtain

$$|\hat{\mathcal{Z}}_{ij}| < \frac{e^{2\lambda_1+2\lambda_2}\, 4^{-2\,m}\, 2^{i+j}\, \lambda_1^i\, \lambda_2^j}{i!\, j!}. \tag{6.16}$$

□

Theorem 6.3. *Under the conditions stated in Theorem 6.2, the truncation error can be estimated as follows:*

$$|\mathcal{Z}(\sigma, t) - \mathcal{Z}_{\mathcal{L}}(\sigma, t)| < \frac{e^{6\,(\lambda_1+\lambda_2)}\, 2^{-2\,m+2\,\mathcal{L}+2} \left(e^{4\,\lambda_1} \lambda_1^{\mathcal{L}+1} + e^{4\,\lambda_2}\, \lambda_2^{\mathcal{L}+1}\right)}{\mathcal{L}!}. \tag{6.17}$$

Proof. In view of the definitions of $\mathcal{Z}(\sigma, t)$ and $\mathcal{Z}_{\mathcal{L}}(\sigma, t)$, we obtain

$$\begin{aligned}
|\mathcal{Z}(\sigma, t) - \mathcal{Z}_{\mathcal{L}}(\sigma, t)| &= \left| \sum_{i=0}^{\infty} \sum_{j=0}^{\infty} \hat{\mathcal{Z}}_{ij}\, \mathrm{F}_i^m(\sigma)\, \mathrm{F}_j^m(t) - \sum_{i=0}^{\mathcal{L}} \sum_{j=0}^{\mathcal{L}} \hat{\mathcal{Z}}_{ij}\, \mathrm{F}_i^m(\sigma)\, \mathrm{F}_j^m(t) \right| \\
&\leq \left| \sum_{i=0}^{\mathcal{L}} \sum_{j=\mathcal{L}+1}^{\infty} \hat{\mathcal{Z}}_{ij}\, \mathrm{F}_i^m(\sigma)\, \mathrm{F}_j^m(t) \right| + \left| \sum_{i=\mathcal{L}+1}^{\infty} \sum_{j=0}^{\infty} \hat{\mathcal{Z}}_{ij}\, \mathrm{F}_i^m(\sigma)\, \mathrm{F}_j^m(t) \right|.
\end{aligned} \tag{6.18}$$

The following expression follows from Theorem 6.2 and Lemma 6.1:

$$\begin{aligned}
&\sum_{i=0}^{\mathcal{L}} \frac{2^{m+i}\, e^{2\,\lambda_1}\, 4^{-m} (2\,\lambda_1)^i}{i!} = \frac{e^{6\lambda_1} 2^{-m} \Gamma(\mathcal{L}+1, 4\lambda_1)}{\mathcal{L}!} < e^{6\,\lambda_1}\, 2^{-m}, \\
&\sum_{j=\mathcal{L}+1}^{\infty} \frac{2^{m+j}\, e^{2\,\lambda_2}\, 4^{-m} (2\,\lambda_2)^j}{j!} = \frac{e^{6\,\lambda_2}\, 2^{-m}\, (\mathcal{L}! - \Gamma(\mathcal{L}+1, 4\,\lambda_2))}{\mathcal{L}!} \\
&\qquad\qquad < \frac{e^{10\,\lambda_2}\, 2^{-m}\, (4\,\lambda_2)^{\mathcal{L}+1}}{\mathcal{L}!}, \\
&\sum_{i=\mathcal{L}+1}^{\infty} = \frac{2^{m+i}\, e^{2\,\lambda_1}\, 4^{-m} (2\,\lambda_1)^i}{i!} = \frac{e^{6\,\lambda_1}\, 2^{-m}\, (\mathcal{L}! - \Gamma(\mathcal{L}+1, 4\,\lambda_1))}{\mathcal{L}!} \\
&\qquad\qquad < \frac{e^{10\,\lambda_1}\, 2^{-m}\, (4\,\lambda_1)^{\mathcal{L}+1}}{\mathcal{L}!}, \\
&\sum_{j=0}^{\infty} \frac{2^{m+j}\, e^{2\,\lambda_2}\, 4^{-m} (2\,\lambda_2)^j}{j!} = e^{6\,\lambda_2}\, 2^{-m}.
\end{aligned} \tag{6.19}$$

Using the estimations and the identity in (6.19), we get the following estimation:

$$|\mathcal{Z}(\sigma,t)-\mathcal{Z}_{\mathcal{L}}(\sigma,t)| < \frac{e^{6\,(\lambda_1+\lambda_2)}\,2^{-2\,m+2\,\mathcal{L}+2}\,\left(e^{4\,\lambda_1}\,\lambda_1^{\mathcal{L}+1}+e^{4\,\lambda_2}\,\lambda_2^{\mathcal{L}+1}\right)}{\mathcal{L}!}. \tag{6.20}$$

□

Theorem 6.4. *(Stability) Let* $\mathcal{Z}_{\mathcal{L}}(\sigma,t)=\sum_{i=0}^{\mathcal{L}}\sum_{j=0}^{\mathcal{L}}\hat{\mathcal{Z}}_{ij}\mathrm{F}_i^m(\sigma)\mathrm{F}_j^m(t)$ *be the approximate solution, and let* $\tilde{\mathcal{Z}}_{\mathcal{L}}(\sigma,t)=\sum_{i=0}^{\mathcal{L}}\sum_{j=0}^{\mathcal{L}}\tilde{\mathcal{Z}}_{ij}\mathrm{F}_i^m(\sigma)\mathrm{F}_j^m(t)$ *denote the numerical solution obtained under a coefficient perturbation that satisfies*

$$|\hat{\mathcal{Z}}_{ij}-\tilde{\mathcal{Z}}_{ij}| \leq \delta\,\frac{e^{2\lambda_1+2\lambda_2}4^{-2m}2^{i+j}\lambda_1^i\lambda_2^j}{i!\,j!}. \tag{6.21}$$

Then the following bound holds*:*

$$\left|\mathcal{Z}_{\mathcal{L}}(\sigma,t)-\tilde{\mathcal{Z}}_{\mathcal{L}}(\sigma,t)\right| < \delta\cdot 4^{-m}e^{6(\lambda_1+\lambda_2)}. \tag{6.22}$$

Proof. Based on the definitions of $\mathcal{Z}_{\mathcal{L}}(\sigma,t)$ and $\tilde{\mathcal{Z}}_{\mathcal{L}}(\sigma,t)$, we can write

$$\mathcal{Z}_{\mathcal{L}}(\sigma,t)-\tilde{\mathcal{Z}}_{\mathcal{L}}(\sigma,t)=\sum_{i=0}^{\mathcal{L}}\sum_{j=0}^{\mathcal{L}}(\hat{\mathcal{Z}}_{ij}-\tilde{\mathcal{Z}}_{ij})\,\mathrm{F}_i^m(\sigma)\,\mathrm{F}_j^m(t), \tag{6.23}$$

which can be rewritten after using the triangle inequality along with Theorem 6.2 and Lemma 6.1 as

$$\begin{aligned}
|\mathcal{Z}_{\mathcal{L}}(\sigma,t)-\tilde{\mathcal{Z}}_{\mathcal{L}}(\sigma,t)| &\leq \sum_{i=0}^{\mathcal{L}}\sum_{j=0}^{\mathcal{L}}|\hat{\mathcal{Z}}_{ij}-\tilde{\mathcal{Z}}_{ij}|\left|\mathrm{F}_i^m(\sigma)\right|\left|\mathrm{F}_j^m(t)\right| \\
&< \sum_{i=0}^{\mathcal{L}}\sum_{j=0}^{\mathcal{L}}\left(\delta\,\frac{e^{2\lambda_1+2\lambda_2}4^{-2m}2^{i+j}\lambda_1^i\lambda_2^j}{i!\,j!}\right)\cdot 2^{i+m}\cdot 2^{j+m} \\
&= \delta\,e^{2\lambda_1+2\lambda_2}4^{-m}\left(\sum_{i=0}^{\mathcal{L}}\frac{(4\lambda_1)^i}{i!}\right)\left(\sum_{j=0}^{\mathcal{L}}\frac{(4\lambda_2)^j}{j!}\right).
\end{aligned} \tag{6.24}$$

With the aid of the inequality

$$\sum_{k=0}^{\mathcal{L}}\frac{\sigma^k}{k!} < e^{\sigma}, \tag{6.25}$$

we get the following desired result:

$$\left|\mathcal{Z}_{\mathcal{L}}(\sigma,t)-\tilde{\mathcal{Z}}_{\mathcal{L}}(\sigma,t)\right| < \delta\cdot 4^{-m}e^{6(\lambda_1+\lambda_2)}. \tag{6.26}$$

□

Remark 6.1. *The convergence results established in this section require sufficient smoothness of the solution and exponential-type bounds on its derivatives. These assumptions may not hold for solutions with limited regularity or singular behavior; in such cases, the spectral convergence rate may deteriorate.*

7. Numerical experiments

In this section, representative numerical examples are presented to verify the accuracy and computational efficiency of the two proposed collocation algorithms for the classical and time-fractional nonlinear fifth-order KdV equations. After implementing the suggested approach, the problem is transformed into a nonlinear algebraic system of dimensions $(\mathcal{L}+1)^2$. This system can be solved using Newton's method, where the initial guess is chosen as 10^{-i+j}, $i, j = 0, \ldots, \mathcal{L}$, and a high working precision of 60 digits is used to ensure convergence to a tolerance of about 10^{-50}. All computations are carried out using the `FindRoot` function in *Mathematica* 11 on an HP Z420 Workstation equipped with an Intel(R) Xeon(R) CPU E5-1620 v2 (3.70 GHz), 16 GB of DDR3 RAM, and 512 GB of storage.

Example 7.1. *[64] We consider the time-fractional NFOKDVEs given in* (5.1) *with*

$$a = 30, \quad b = 20, \quad d = 10.$$

The functions appearing on the right-hand side of the conditions (4.2)–(4.4) are specified as

$$f(\sigma) = 2k^2(3\tanh(k\,\sigma_0 - k\sigma) + 2), \tag{7.1}$$

$$h_0(t) = 2k^2\left(3\tanh\left(k\,\sigma_0 + 56\,k^5\,t\right) + 2\right), \tag{7.2}$$

$$h_1(t) = 2k^2\left(2 - 3\tanh\left(-k\,\sigma_0 - 56\,k^5\,t + k\right)\right), \tag{7.3}$$

$$h_2(t) = -\,6k^3\,\mathrm{sech}^2\left(k\,\sigma_0 + 56\,k^5\,t\right), \tag{7.4}$$

$$h_3(t) = -\,6k^3\,\mathrm{sech}^2\left(-k\,\sigma_0 - 56\,k^5\,t + k\right), \tag{7.5}$$

$$h_4(t) = -\,12k^4\tanh\left(k\,\sigma_0 + 56\,k^5\,t\right)\mathrm{sech}^2\left(k\,\sigma_0 + 56\,k^5 t\right). \tag{7.6}$$

The exact solution at $\beta = 1$ is given by

$$\mathcal{Z}(\sigma, t) = 2k^2\left(2 - 3\tanh\left(k\,\sigma - 56\,k^5\,t - k\,\sigma_0\right)\right).$$

Table 1 compares the CPU time used (in seconds) and L^∞ errors obtained by the present algorithm with those reported in [64] for $\beta = 1$, $k = 0.01$, and $\sigma_0 = 0$. The pointwise absolute errors (AEs) for $m = 4$ at several times are displayed in Figure 1. Figure 2 reports the behavior of the L_2 and L_∞ errors as $\mathcal{L}$ varies when $m = 8$ and $k = 0.1$. Table 2 lists the CPU time (in seconds) used and AEs for $m = 11$, $k = 0.1$, and $\mathcal{L} = 9$, while Figure 3 shows the effect of changing $\mathcal{L}$ for $m = 2$ and $k = 0.1$. Residual errors for different fractional orders and levels are given in Table 3, and Figure 4 depicts the residual behavior for $\beta = 0.5$, $m = 3$, and $k = 0.001$. *Finally, Table 4 presents a comparison of L^∞ errors at $\beta = 1$, between the proposed method and method in [67].*

Table 1. L^∞ errors for Example 7.1 at $\beta = 1$.

Method in [64]				Proposed method			
$\left(2\hat{M}, \Delta t\right)$	$\left(64, \frac{1}{10}\right)$	$\left(64, \frac{1}{100}\right)$	$\left(64, \frac{1}{1000}\right)$	$(\mathcal{L}, m)$	$(6, 1)$	$(6, 2)$	$(7, 15)$
Error	3.0045×10^{-7}	3.0055×10^{-8}	3.0198×10^{-9}	Error	8.61941×10^{-18}	9.21572×10^{-19}	1.02999×10^{-18}
CPU time	0.040135	0.232144	1.893176		5.407	5.875	8.344

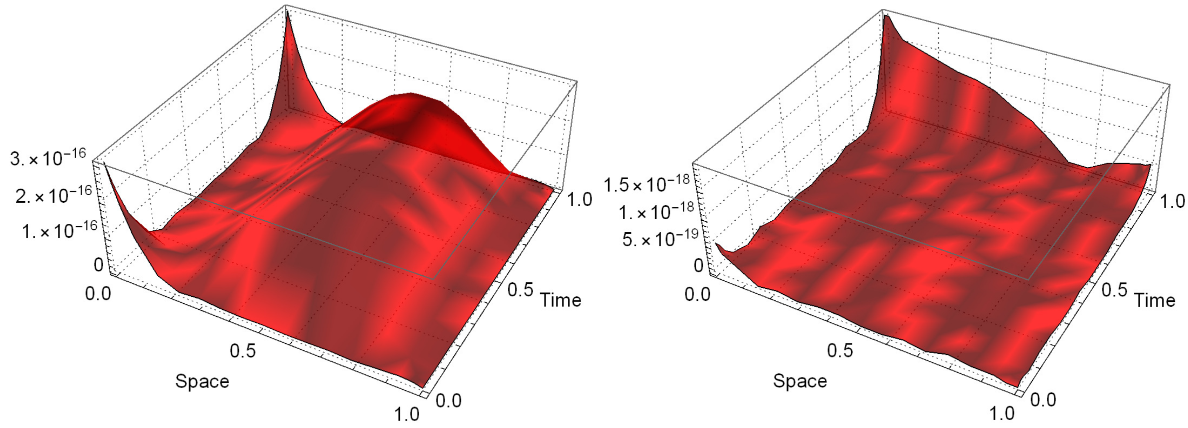

(a) $\mathcal{L} = 4$. **(b)** $\mathcal{L} = 5$.

Figure 1. AEs for Example 7.1 at $\beta = 1$ and $m = 4$.

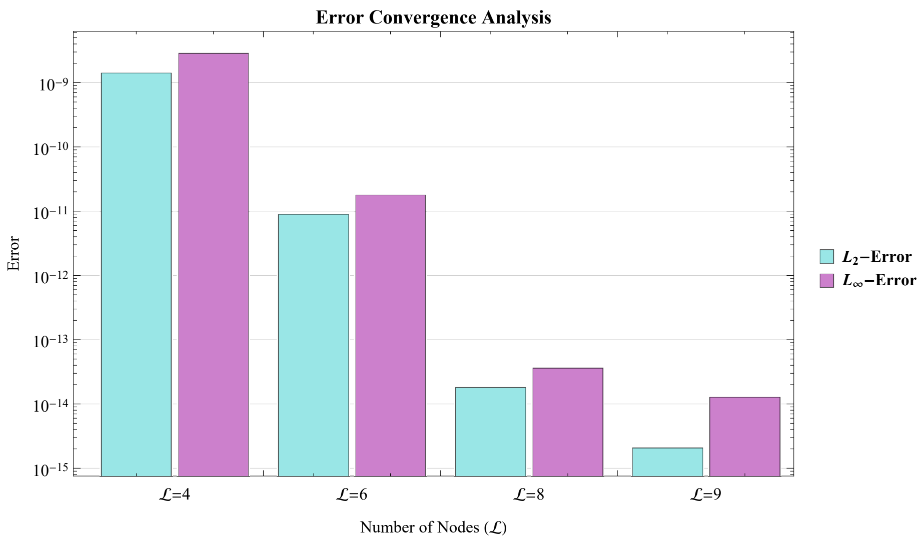

Figure 2. L_2 and L_∞ errors for Example 7.1 at $\beta = 1$, $m = 8$, and $k = 0.1$.

Table 2. AEs for Example 7.1 at $\beta = 1$, $m = 11$, $k = 0.1$, and $\mathcal{L} = 9$.

σ	$t = 0.3$	$t = 0.6$	$t = 0.9$	CPU time
0.1	6.93889×10^{-18}	6.93889×10^{-18}	0	
0.2	2.77556×10^{-17}	2.77556×10^{-17}	2.08167×10^{-17}	
0.3	7.63278×10^{-17}	8.32667×10^{-17}	6.93889×10^{-17}	
0.4	1.59595×10^{-16}	1.52656×10^{-16}	1.52656×10^{-16}	
0.5	2.56739×10^{-16}	2.498×10^{-16}	2.49812×10^{-16}	17.781
0.6	3.33067×10^{-16}	3.26128×10^{-16}	3.33067×10^{-16}	
0.7	3.81639×10^{-16}	3.81639×10^{-16}	3.88578×10^{-16}	
0.8	3.05311×10^{-16}	3.1225×10^{-16}	3.05311×10^{-16}	
0.9	1.52656×10^{-16}	1.52656×10^{-16}	1.11022×10^{-16}	

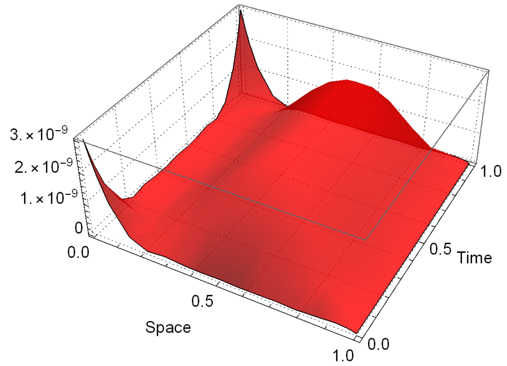

(a) $\mathcal{L} = 4$.

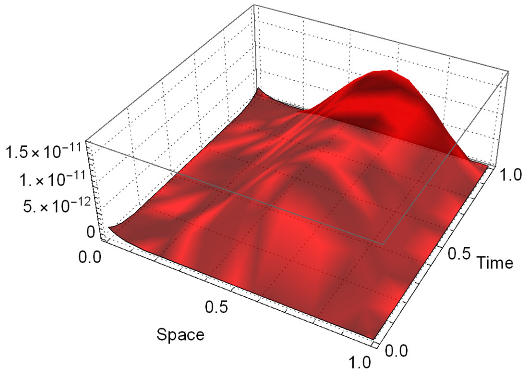

(b) $\mathcal{L} = 6$.

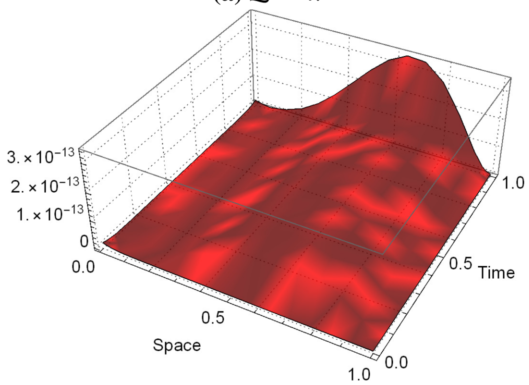

(c) $\mathcal{L} = 7$.

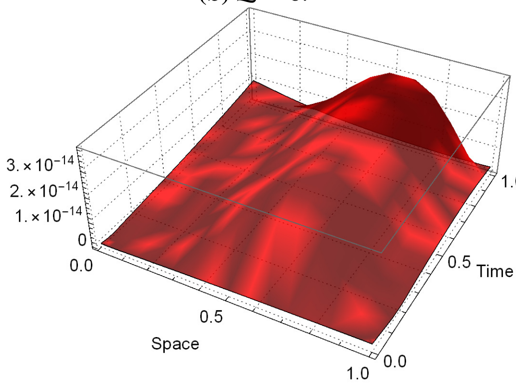

(d) $\mathcal{L} = 8$.

Figure 3. AEs for Example 7.1 at $\beta = 1$, $m = 2$, and $k = 0.1$.

Table 3. Residual AEs $\left|\mathcal{R}^2_{\mathcal{L}}(\sigma, t)\right|$ of Example 7.1 at $k = 0.001$ and $\mathcal{L} = 8$.

$\sigma = t$	$\beta = 0.1$, $m = 2$	$\beta = 0.4$, $m = 6$	$\beta = 0.8$, $m = 14$
0.1	4.10143×10^{-13}	4.06871×10^{-13}	3.84906×10^{-13}
0.2	1.13639×10^{-13}	1.12573×10^{-13}	1.06402×10^{-13}
0.3	4.93103×10^{-14}	4.90703×10^{-14}	4.60656×10^{-14}
0.4	3.11446×10^{-14}	3.02578×10^{-14}	2.85787×10^{-14}
0.5	2.53174×10^{-14}	2.61909×10^{-14}	2.444×10^{-14}
0.6	3.21092×10^{-14}	2.97889×10^{-14}	2.82573×10^{-14}
0.7	4.63266×10^{-14}	4.90509×10^{-14}	4.54735×10^{-14}
0.8	1.15×10^{-13}	1.08519×10^{-13}	1.02409×10^{-13}
0.9	3.79608×10^{-13}	3.84437×10^{-13}	3.61464×10^{-13}

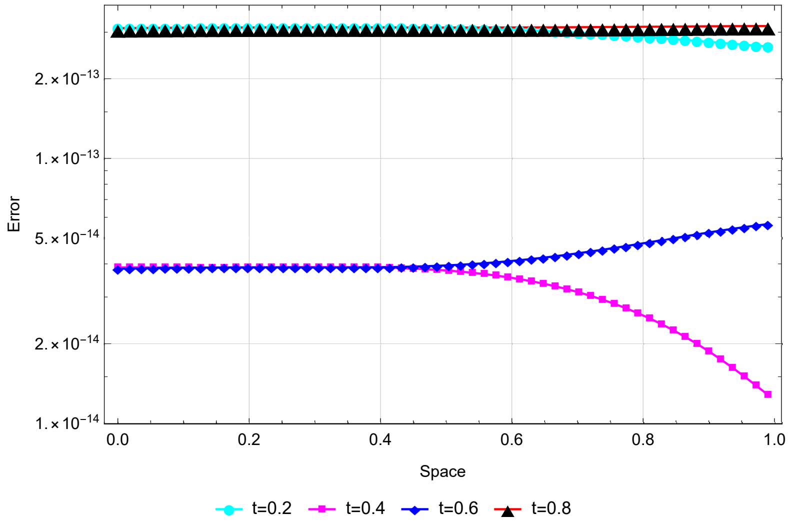

(a) $\mathcal{L} = 7$.

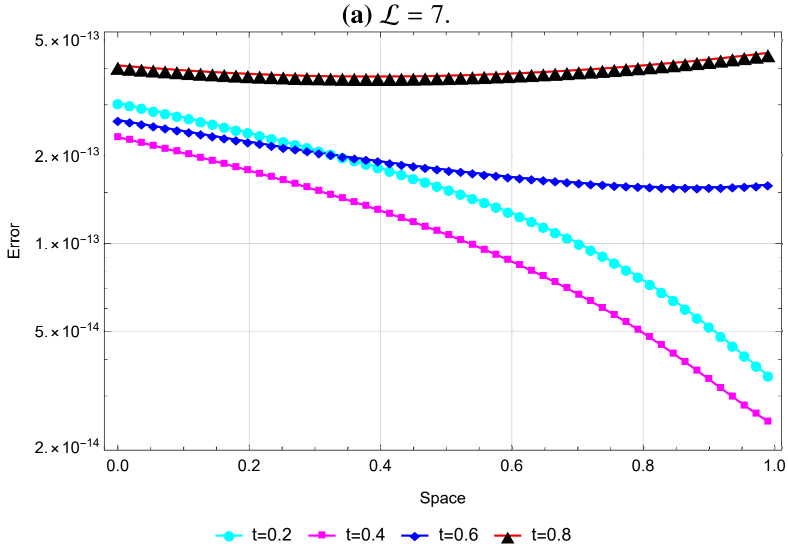

(b) $\mathcal{L} = 8$.

Figure 4. Residual AEs $\left|\mathcal{R}^2_{\mathcal{L}}(\sigma, t)\right|$ of Example 7.1 at $\beta = 0.5$, $m = 3$, and $k = 0.001$.

Table 4. L^∞ errors for Example 7.1 at $\beta = 1$.

	Method in [67] at $N = 12$	Proposed method at $(\mathcal{L}, m) = (6, 2)$
Error	1.06572×10^{-15}	9.21572×10^{-19}

Example 7.2. *[64] We consider the time-fractional NFOKDVEs given in* (5.1) *with*

$$a = 45, \quad b = 15, \quad d = 15.$$

The functions appearing on the right-hand side of the conditions (4.2)–(4.4) are specified as

$$f(\sigma) = 2k^2 \operatorname{sech}^2(k\,\sigma_0 - k\sigma), \tag{7.7}$$

$$h_0(t) = 2k^2 \operatorname{sech}^2\left(k\,\sigma_0 + 16k^5 t\right), \tag{7.8}$$

$$h_1(t) = 2k^2\,\mathrm{sech}^2\Big(-k\,\sigma_0 - 16k^5 t + k\Big), \tag{7.9}$$
$$h_2(t) = 4k^3\tanh\Big(k\left(\sigma_0 + 16k^4 t\right)\Big)\,\mathrm{sech}^2\Big(k\left(\sigma_0 + 16k^4 t\right)\Big), \tag{7.10}$$
$$h_3(t) = -4k^3\tanh\Big(-k\,\sigma_0 - 16k^5 t + k\Big)\,\mathrm{sech}^2\Big(k\left(\sigma_0 + 16k^4 t - 1\right)\Big), \tag{7.11}$$
$$h_4(t) = 4k^4\left(\cosh\Big(2k\left(\sigma_0 + 16k^4 t\right)\Big) - 2\right)\mathrm{sech}^4\Big(k\left(\sigma_0 + 16k^4 t\right)\Big). \tag{7.12}$$

The exact solution at $\beta = 1$ is given by

$$\mathcal{Z}(\sigma, t) = 2\,k^2\,\mathrm{sech}^2\left(k\,\sigma - 16\,k^5\,t - k\,\sigma_0\right).$$

Table 5 presents a comparison of the CPU time used and L^∞ error between the proposed method and the method in [64] when $\beta = 1$, $k = 0.2$, and $\sigma_0 = 0$. Figure 5 shows the L_2 and L_∞ errors at $\beta = 1$ and different values of $\mathcal{L}$ when $m = 9$ and $k = 0.2$. Table 6 reports the CPU time used (in seconds) and AEs at $\beta = 1$ and various values of t when $m = 5$, $k = 0.2$, and $\mathcal{L} = 8$. Table 7 reports the residual AEs $\left|\mathcal{R}^2_{\mathcal{L}}(\sigma, t)\right|$ at different values of β, m, and $\mathcal{L}$ when $k = 0.2$. Table 8 presents the L^∞ errors at different values of m when $\beta = 1$, $k = 0.2$, and $\mathcal{L} = 10$. Figure 6 illustrates the residual AEs $\left|\mathcal{R}^2_{\mathcal{L}}(\sigma, t)\right|$ at different values of $\mathcal{L}$ when $\beta = 0.2$, $m = 5$, and $k = 0.2$.

Table 5. L^∞ errors for Example 7.2 at $\beta = 1$.

Method in [64]				Proposed method			
$(2\hat{M}, \Delta t)$	$(64, \frac{1}{10})$	$(64, \frac{1}{100})$	$(64, \frac{1}{1000})$	$(\mathcal{L}, m)$	$(8, 2)$	$(10, 10)$	$(10, 17)$
Error	7.793×10^{-9}	7.039×10^{-10}	5.937×10^{-12}	Error	7.348×10^{-11}	5.935×10^{-13}	1.644×10^{-12}
CPU time	0.047167	0.227436	1.924651		11.813	27.046	27.811

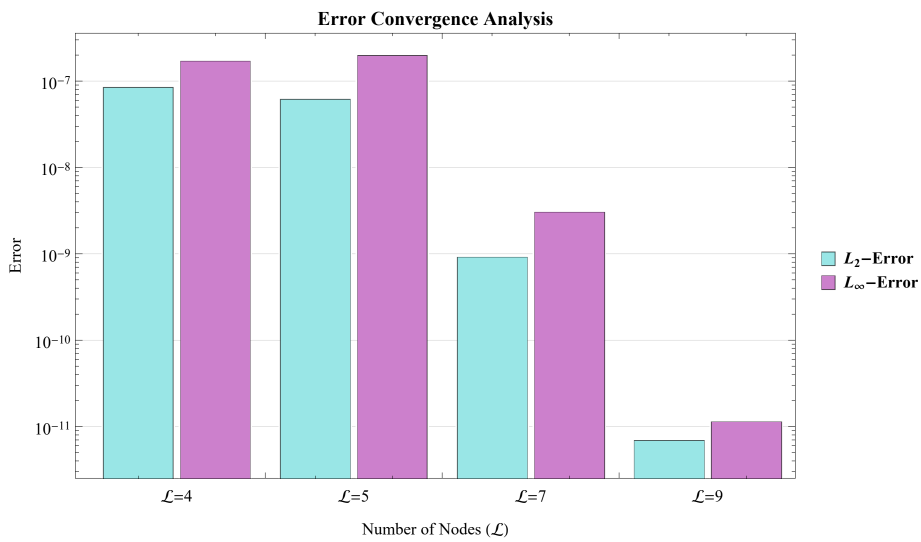

Figure 5. L_2 and L_∞ errors for Example 7.2 at $\beta = 1$, $m = 9$, and $k = 0.2$.

Table 6. AEs for Example 7.2 at $\beta = 1$, $m = 5$, $k = 0.2$, and $\mathcal{L} = 8$.

σ	$t = 0.3$	$t = 0.6$	$t = 0.9$	CPU time
0.1	8.64364×10^{-13}	8.50847×10^{-13}	8.18776×10^{-13}	
0.2	6.04702×10^{-12}	5.95075×10^{-12}	5.7306×10^{-12}	
0.3	1.75067×10^{-11}	1.72284×10^{-11}	1.65897×10^{-11}	
0.4	3.46223×10^{-11}	3.40726×10^{-11}	3.28092×10^{-11}	
0.5	5.41998×10^{-11}	5.33408×10^{-11}	5.13625×10^{-11}	11.955
0.6	7.05117×10^{-11}	6.93973×10^{-11}	6.68239×10^{-11}	
0.7	7.56296×10^{-11}	7.44401×10^{-11}	7.16818×10^{-11}	
0.8	6.14684×10^{-11}	6.05091×10^{-11}	5.8272×10^{-11}	
0.9	2.72762×10^{-11}	2.68556×10^{-11}	2.58669×10^{-11}	

Table 7. Residual AEs $\left|\mathcal{R}^2_{\mathcal{L}}(\sigma, t)\right|$ of Example 7.2 at $k = 0.2$.

$\sigma = t$	$\beta = 0.25,\ m = 1,\ \mathcal{L} = 6$	$\beta = 0.45,\ m = 2,\ \mathcal{L} = 8$	$\beta = 0.95,\ m = 3,\ \mathcal{L} = 9$
0.1	8.80158×10^{-6}	2.12066×10^{-7}	2.26425×10^{-10}
0.2	2.46322×10^{-6}	1.30393×10^{-7}	3.46352×10^{-10}
0.3	5.89214×10^{-7}	8.55827×10^{-8}	4.55133×10^{-10}
0.4	5.98651×10^{-6}	6.78922×10^{-8}	5.76367×10^{-10}
0.5	1.67212×10^{-5}	4.33037×10^{-8}	7.27837×10^{-10}
0.6	3.58870×10^{-5}	3.88306×10^{-7}	2.39464×10^{-8}
0.7	6.36423×10^{-5}	8.26358×10^{-7}	1.46419×10^{-7}
0.8	1.00932×10^{-4}	3.25409×10^{-6}	5.08665×10^{-7}
0.9	1.57195×10^{-4}	3.91380×10^{-6}	1.34750×10^{-6}

Table 8. L^∞ errors of Example 7.2 at $\beta = 1$ and $\mathcal{L} = 10$.

m	4	6	9
Error	6.96534×10^{-1}	1.18346×10^{-6}	6.04489×10^{-13}

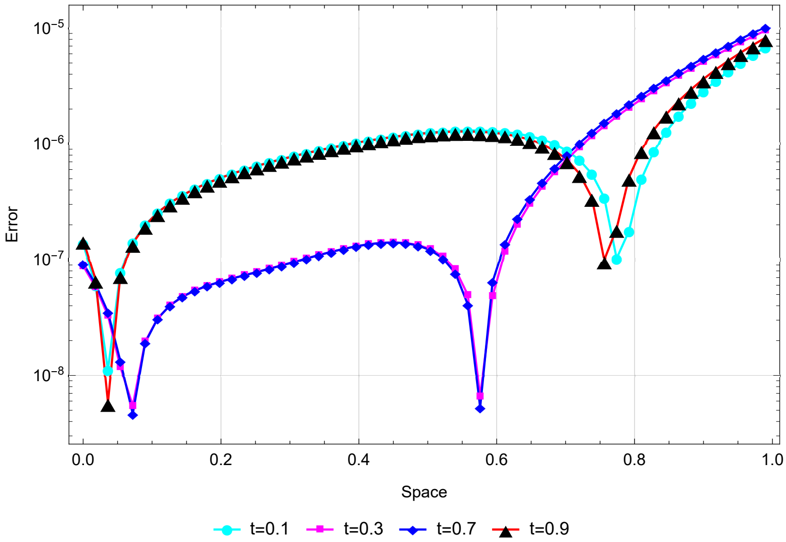

(a) $\mathcal{L} = 8$.

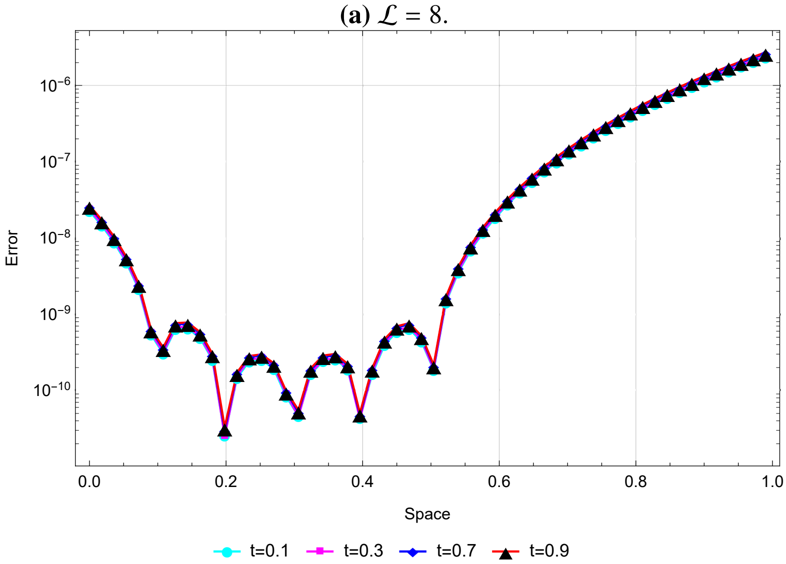

(b) $\mathcal{L} = 9$.

Figure 6. Residual AEs $\left|\mathcal{R}^2_{\mathcal{L}}(\sigma, t)\right|$ of Example 7.2 at $\beta = 0.2$, $m = 5$, and $k = 0.2$.

Remark 7.1. *It is worth mentioning here that, for a fixed* $\mathcal{L} = 10$*, increasing the level parameter* m *significantly improves the* L^∞ *accuracy, as demonstrated in Table 8. This exponential error reduction occurs because larger values of* m *adjust the degree spacing of the expansion functions* $\mathrm{F}_i^m(\sigma)$*, enabling the basis space to approximate fifth-order spatial derivatives with high structural fidelity without increasing the dimension* $\mathcal{L}$.

Example 7.3. *[64] We consider the time-fractional NFOKDVEs given in* (5.1) *with*

$$a = 2, \quad b = 6, \quad d = 3.$$

The functions appearing on the right-hand side of the conditions (4.2)–(4.4) are specified as

$$f(\sigma) = 10k^2\left(2 - 3\tanh^2(k(\sigma_0 + \sigma))\right), \tag{7.13}$$

$$
\begin{aligned}
h_0(t) =& 10k^2 \left(2 - 3\tanh^2\left(k\left(\sigma_0 - 96k^4 t\right)\right)\right), && (7.14)\\
h_1(t) =& 10k^2 \left(2 - 3\tanh^2\left(k\sigma_0 - 96k^5 t + k\right)\right), && (7.15)\\
h_2(t) =& -60k^3 \tanh\left(k\left(\sigma_0 - 96k^4 t\right)\right)\operatorname{sech}^2\left(k\left(\sigma_0 - 96k^4 t\right)\right), && (7.16)\\
h_3(t) =& -60k^3 \tanh\left(k\sigma_0 - 96k^5 t + k\right)\operatorname{sech}^2\left(k\sigma_0 - 96k^5 t + k\right), && (7.17)\\
h_4(t) =& 60k^4 \left(\cosh\left(2k\left(\sigma_0 - 96k^4 t\right)\right) - 2\right)\operatorname{sech}^4\left(k\left(\sigma_0 - 96k^4 t\right)\right). && (7.18)
\end{aligned}
$$

The exact solution at $\beta = 1$ is given by

$$\mathcal{Z}(\sigma, t) = 20\,k^2 - 30\,k^2 \tanh^2\left(k\,\sigma - 96\,k^5\,t + k\,\sigma_0\right).$$

Table 9 compares the CPU time used and L^∞ errors obtained by the proposed method with those reported in [64] for $\beta = 1$, $k = 0.12$, and $\sigma_0 = 0$. Figure 7 depicts the corresponding L_2 and L_∞ errors for $\beta = 1$, $m = 18$, and $k = 0.12$. Table 10 lists the CPU time used and AEs at various values of t for $\beta = 1$, $m = 5$, $k = 0.12$, and $\mathcal{L} = 9$. The approximate solution and the associated AEs are displayed in Figure 8 for $\beta = 1$ and $m = 12$. Furthermore, Table 11 reports the residual absolute errors $\left|\mathcal{R}^2_{\mathcal{L}}(\sigma, t)\right|$ for different values of β and m when $k = 0.12$ and $\mathcal{L} = 9$. Finally, Figure 9 illustrates the residual absolute errors $\left|\mathcal{R}^2_{\mathcal{L}}(\sigma, t)\right|$ for various values of $\mathcal{L}$ with $\beta = 0.9$, $m = 30$, and $k = 0.12$. At $\beta = 1$, $m = 4$, and $k = 0.12$, Figures 10 and 11 show the convergence rate of L_2 and L_∞ errors at different values of $\mathcal{L}$ and $|\mathcal{Z}_{\mathcal{L}+1}(\sigma, t) - \mathcal{Z}_{\mathcal{L}}(\sigma, t)|$ when $\sigma = t$, respectively.

Table 9. L^∞ errors for Example 7.3 at $\beta = 1$.

Method in [64]				Proposed method		
$\left(2\hat{M}, \Delta t\right)$	$\left(64, \frac{1}{10}\right)$	$\left(64, \frac{1}{100}\right)$	$\left(64, \frac{1}{1000}\right)$	$(m, \mathcal{L})$	$(8, 2)$	$(9, 9)$
Error	4.4562×10^{-6}	4.3726×10^{-7}	4.4826×10^{-8}	Error	2.47949×10^{-12}	4.12765×10^{-13}
CPU time	0.050296	0.212037	1.968975		12.158	17.892

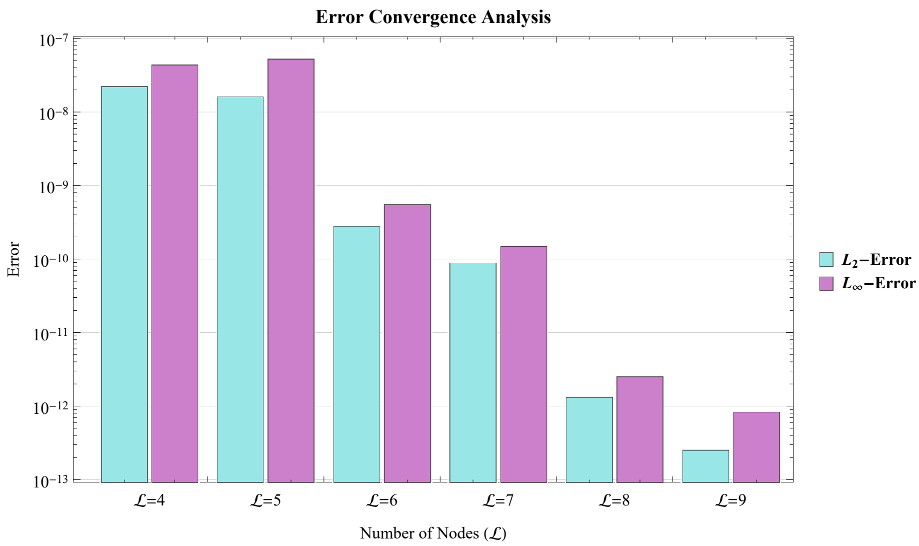

Figure 7. L_2 and L_∞ errors for Example 7.3 at $\beta = 1$, $m = 18$, and $k = 0.12$.

Table 10. AEs for Example 7.3 at $\beta = 1$, $m = 5$, $k = 0.12$, and $\mathcal{L} = 9$.

σ	$t = 0.2$	$t = 0.4$	$t = 0.6$	$t = 0.8$	CPU time
0.1	1.38223×10^{-14}	2.55906×10^{-14}	5.16809×10^{-14}	9.32587×10^{-14}	
0.2	1.81521×10^{-14}	2.49800×10^{-15}	3.75810×10^{-14}	8.50431×10^{-14}	
0.3	8.50986×10^{-14}	5.56222×10^{-14}	1.21014×10^{-14}	3.92464×10^{-14}	
0.4	1.84353×10^{-13}	1.45883×10^{-13}	9.41469×10^{-14}	4.03566×10^{-14}	
0.5	2.99483×10^{-13}	2.51354×10^{-13}	1.90958×10^{-13}	1.35503×10^{-13}	19.297
0.6	4.01512×10^{-13}	3.42559×10^{-13}	2.72449×10^{-13}	2.14773×10^{-13}	
0.7	4.49141×10^{-13}	3.77254×10^{-13}	2.95153×10^{-13}	2.33313×10^{-13}	
0.8	3.95795×10^{-13}	3.07754×10^{-13}	2.09832×10^{-13}	1.39999×10^{-13}	
0.9	2.26319×10^{-13}	1.17628×10^{-13}	1.94289×10^{-15}	8.60978×10^{-14}	

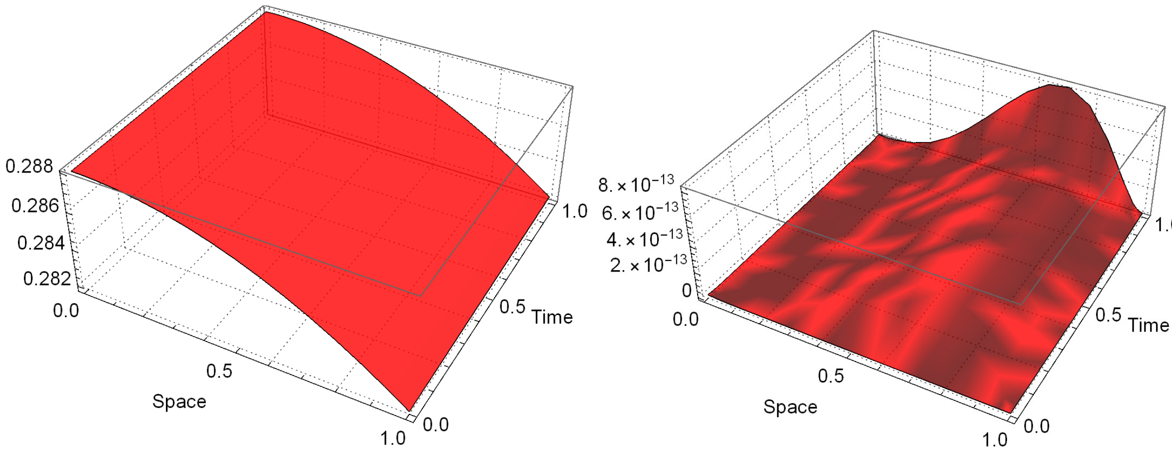

(a) Solution. **(b)** Error.

Figure 8. Approximate solution (left) and absolute-error surface (right) for Example 7.3 at $\beta = 1$ and $m = 12$.

Table 11. Residual AEs $\left|\mathcal{R}^2_{\mathcal{L}}(\sigma, t)\right|$ of Example 7.3 at $k = 0.12$ and $\mathcal{L} = 9$.

$\sigma = t$	$\beta = 0.2$, $m = 2$	$\beta = 0.5$, $m = 7$	$\beta = 0.7$, $m = 10$
0.1	9.47322×10^{-18}	1.51286×10^{-12}	2.37069×10^{-12}
0.2	1.41844×10^{-16}	1.90104×10^{-12}	5.39586×10^{-12}
0.3	1.07877×10^{-15}	6.56689×10^{-12}	8.9281×10^{-12}
0.4	4.60081×10^{-15}	1.2623×10^{-11}	1.27773×10^{-11}
0.5	1.35513×10^{-14}	2.0002×10^{-11}	1.67316×10^{-11}
0.6	4.17733×10^{-10}	2.0702×10^{-10}	1.99578×10^{-10}
0.7	3.46561×10^{-9}	2.30212×10^{-9}	2.29181×10^{-9}
0.8	1.4217×10^{-8}	1.13655×10^{-8}	1.13593×10^{-8}
0.9	5.67561×10^{-8}	4.49721×10^{-8}	4.49888×10^{-8}

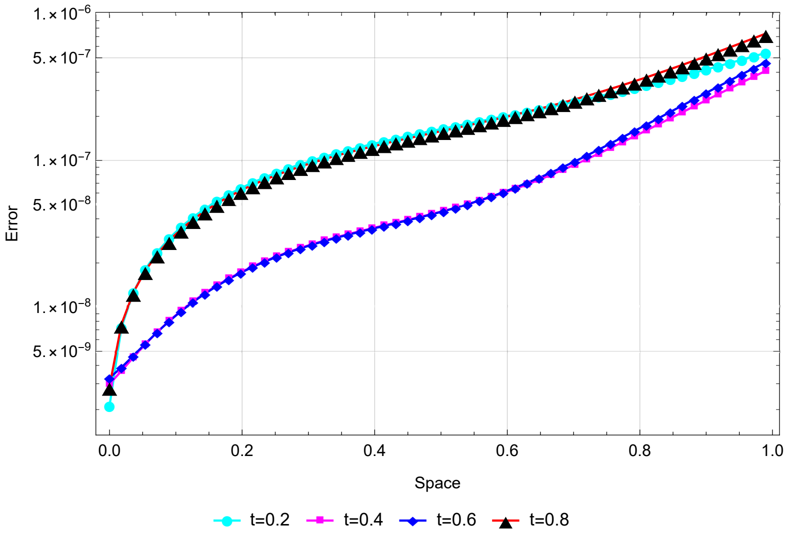

(a) $\mathcal{L} = 8$.

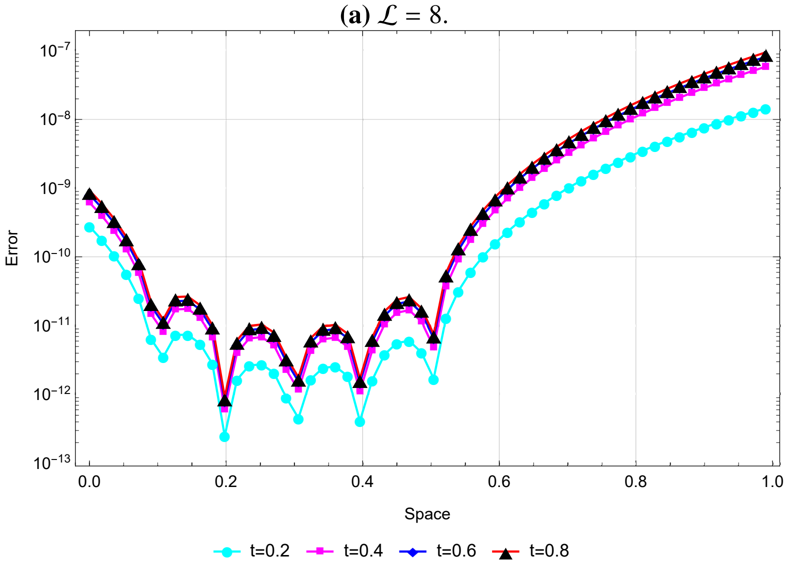

(b) $\mathcal{L} = 9$.

Figure 9. Residual AEs $\left|\mathcal{R}^2_{\mathcal{L}}(\sigma, t)\right|$ of Example 7.3 at $\beta = 0.9$, $m = 30$, and $k = 0.12$.

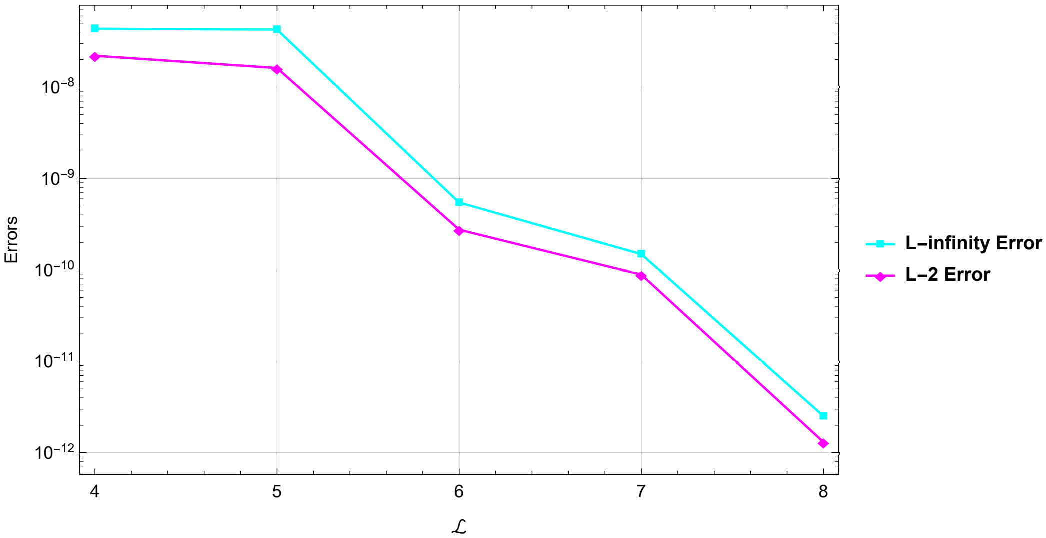

Figure 10. Convergence rate of L_2 and L_∞ errors for Example 7.3 at $\beta = 1$, $m = 4$, and $k = 0.12$.

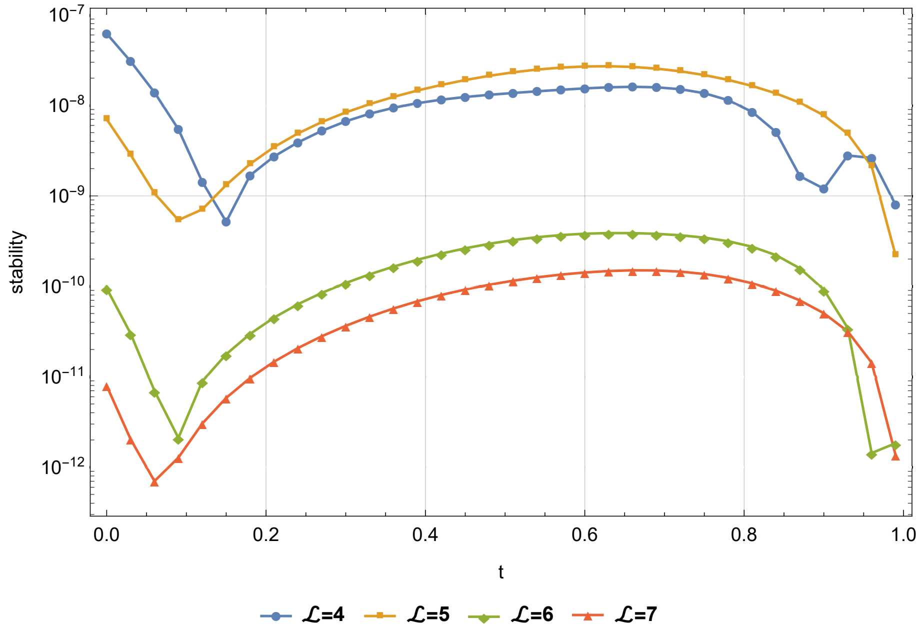

Figure 11. $|\mathcal{Z}_{\mathcal{L}+1}(\sigma, t) - \mathcal{Z}_{\mathcal{L}}(\sigma, t)|$ for Example 7.3 when $\sigma = t$ at $\beta = 1$, $m = 4$, and $k = 0.12$.

Example 7.4. *We consider the time-fractional NFOKDVEs given in* (5.1) *with*

$$a = b = d = 1.$$

The functions appearing on the right-hand side of the conditions (4.2)–(4.4) are specified as

$$f(\sigma) = 10^{-3}\,\sigma^3(1-\sigma)^2, \tag{7.19}$$
$$h_0(t) = h_1(t) = h_2(t) = h_3(t) = h_4(t) = 0. \tag{7.20}$$

Since the exact solution is not available, we define the following absolute residual error norm

$$RE = \max_{0\le\sigma,t\le1} \left| \frac{\partial^\beta \mathcal{Z}(\sigma,t)}{\partial t^\beta} + \mathcal{Z}(\sigma,t)^2 \left(\frac{\partial \mathcal{Z}(\sigma,t)}{\partial \sigma}\right) + \left(\frac{\partial \mathcal{Z}(\sigma,t)}{\partial \sigma}\right)\left(\frac{\partial^2 \mathcal{Z}(\sigma,t)}{\partial \sigma^2}\right) \right. \\ \left. + \mathcal{Z}(\sigma,t)\left(\frac{\partial^3 \mathcal{Z}(\sigma,t)}{\partial \sigma^3}\right) + \frac{\partial^5 \mathcal{Z}(\sigma,t)}{\partial \sigma^5} \right|, \tag{7.21}$$

and apply the proposed method at different values of t when $\beta = 0.5$, $m = 30$, and $\mathcal{L} = 4$ to get Table 12, which illustrates the residual error at different values of σ.

Table 12. Residual error of Example 7.4 at $\beta = 0.5$, $m = 30$, and $\mathcal{L} = 4$.

x	$t = 0.1$	$t = 0.3$	$t = 0.7$	$t = 0.9$
0.1	2.32497×10^{-5}	1.29848×10^{-5}	8.61061×10^{-6}	5.98037×10^{-6}
0.2	1.15865×10^{-5}	6.47943×10^{-6}	4.29659×10^{-6}	3.00003×10^{-6}
0.3	2.75638×10^{-5}	1.54140×10^{-5}	1.02212×10^{-5}	7.13624×10^{-6}
0.4	5.21433×10^{-5}	2.91575×10^{-5}	1.93348×10^{-5}	1.34962×10^{-5}
0.5	7.17368×10^{-5}	4.01168×10^{-5}	2.66020×10^{-5}	1.85745×10^{-5}
0.6	7.81993×10^{-5}	4.37359×10^{-5}	2.90018×10^{-5}	2.02598×10^{-5}
0.7	6.88232×10^{-5}	3.84966×10^{-5}	2.55275×10^{-5}	1.78414×10^{-5}
0.8	4.63311×10^{-5}	2.59174×10^{-5}	1.71861×10^{-5}	1.20151×10^{-5}
0.9	1.88697×10^{-5}	1.05543×10^{-5}	6.99867×10^{-6}	4.89042×10^{-6}

Remark 7.2. *As with standard spectral methods, the condition number grows in a polynomial-like manner as $\mathcal{L}$ increases. However, the proposed basis mitigates this growth, keeping this condition number manageable for practical choices of $\mathcal{L} \le 10$. To reduce round-off sensitivity during matrix inversion, we performed the computations using an extended working precision of* 60 *decimal digits in Wolfram Mathematica.*

Remark 7.3. *Figure 12 shows the theoretical stability bounds as a function of the perturbation magnitude δ across different Fibonacci level parameters m. This bound is independent of $\mathcal{L}$. This indicates that the proposed scheme remains stable under δ as $\mathcal{L}$ increases.*

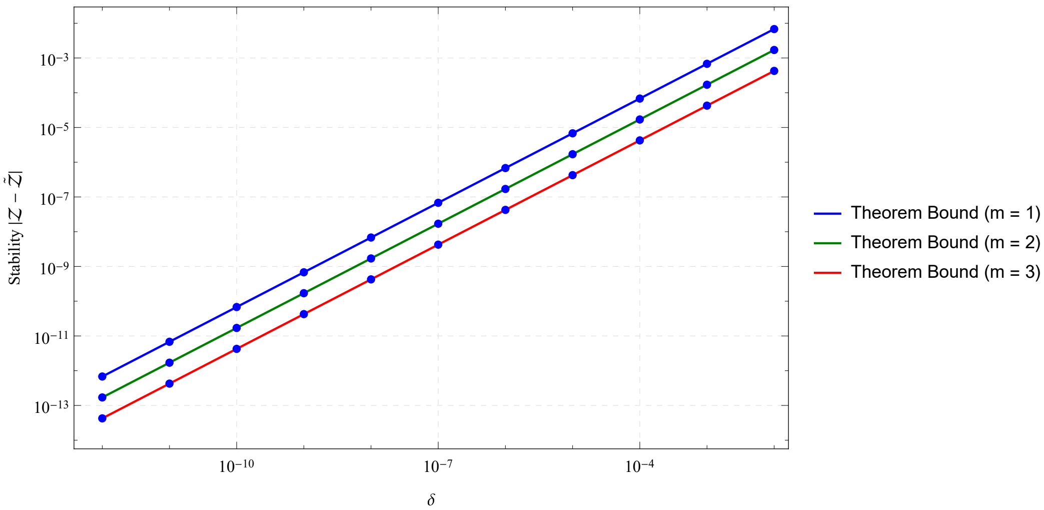

Figure 12. Stability $|\mathcal{Z}_{\mathcal{L}+1}(\sigma, t) - \mathcal{Z}_{\mathcal{L}}(\sigma, t)|$.

Remark 7.4. *To balance accuracy and computational cost, $\mathcal{L}$ is chosen according to the desired accuracy and computational cost, while m is tuned to enhance the approximation accuracy without changing the dimension of the algebraic system. An appropriate combination of $(\mathcal{L}, m)$ therefore provides a balance between accuracy and computational cost.*

8. Final remarks

This paper presented spectral-collocation algorithms for the classical and time-fractional nonlinear fifth-order KdV equations by employing Fibonacci level m polynomials as trial functions. The construction required several new analytical ingredients for this polynomial family. In particular, an inversion formula was proved and then used to obtain integer- and fractional-order derivative representations, along with the associated operational matrices. The derived matrices were incorporated into the collocation discretization of the considered nonlinear models. As a result, the differential problems were reduced to nonlinear algebraic systems for the unknown expansion coefficients. These systems were solved by Newton's iterative method. The numerical experiments, comparison studies, and residual error analyses confirm the accuracy and efficiency of the proposed algorithms, showing that highly accurate approximations can be achieved with relatively small values of $\mathcal{L}$. The results also showed that the level parameter m provides additional flexibility in constructing effective polynomial bases for these nonlinear wave models. To the best of our knowledge, this is the first use of Fibonacci level m polynomials in numerical analysis and spectral-collocation methods. The encouraging performance obtained here suggests several possible extensions. Future work may apply these polynomials to other ordinary, partial, integro-differential, delay, and fractional DEs, especially models arising in fluid mechanics, mathematical physics, engineering, and other applied sciences.

Author contributions

Mohamed Adel: Validation, investigation, funding acquisition; Ahmed Gamal Atta: Conceptualization, methodology, software, validation, formal analysis, investigation, writing—

original draft preparation, writing—reviewing and editing; Naher Mohammed A. Alsafri: Methodology, validation, investigation; Mohamed Abbas El-Naggar: Validation, investigation; Waleed Mohamed Abd-Elhameed: Conceptualization, methodology, software, validation, formal analysis, writing—original draft preparation, writing—reviewing and editing, supervision. All authors have read and approved the final version of the manuscript for publication.

Use of Generative-AI tools declaration

The authors declare that they have not used Artificial Intelligence (AI) tools in the creation of this article.

Acknowledgments

The authors extend their appreciation to the Deanship of Scientific Research, Islamic University of Madinah, Saudi Arabia, for funding this research work.

Conflict of interest

The authors declare that they have no competing interests.

References

1. R. C. Koeller, Applications of fractional calculus to the theory of viscoelasticity, *J. Appl. Mech.*, **51** (1984), 299–307. https://doi.org/10.1115/1.3167616
2. K. B. Oldham, J. Spanier, *The fractional calculus: theory and applications of differentiation and integration to arbitrary order*, New York: Academic Press, 1974
3. A. A. Kilbas, H. M. Srivastava, J. J. Trujillo, *Theory and applications of fractional differential equations*, Amsterdam: Elsevier, 2006
4. Y. Li, Z. H. Rui, B. Hu, Monotone iterative and quasilinearization method for a nonlinear integral impulsive differential equation, *AIMS Math.*, **10** (2025), 21–37. https://doi.org/https://doi.org/10.3934/math.2025002
5. B. Hu, Y. K. Liao, Convergence conditions for extreme solutions of an impulsive differential system, *AIMS Math.*, **10** (2025), 10591–10604. https://doi.org/https://doi.org/10.3934/math.2025481
6. D. Damircheli, M. Razzaghi, Time-space collocation based on fractional-order generalized Chebyshev wavelets for fractional advection problem, *J. Comput. Appl. Math.*, **488** (2026), 117776. https://doi.org/10.1016/j.cam.2026.117776
7. M. Hossain, M. A. Ullah, A new hybrid Laplace Adomian variational iteration method for solving nonlinear time-fractional partial differential equations, *Ann. Univ. Ferrara*, **72** (2026), 37. https://doi.org/10.1007/s11565-026-00658-9

8. P. E. Kloeden, D. T. Son, H. T. Tuan, Lyapunov methods for dissipative Caputo fractional differential equations with two indices, *Commun. Nonlinear Sci.*, **157** (2026), 109737. https://doi.org/10.1016/j.cnsns.2026.109737

9. M. Boumaaza, A. Boutiara, O. Djidel, R. Guefaifia, S. Boulaaras, Analysis of delay differential equations with dual Caputo-type fractional derivatives using Laplace transform methods, *Sci. Rep.*, **16** (2026), 11181. https://doi.org/10.1038/s41598-026-41584-2

10. Z. W. Wang, Y. G. Zhu, Optimal control method for uncertain fractional switched systems and application to glucose-insulin regulatory, *Commun. Nonlinear Sci.*, **159** (2026), 109900. https://doi.org/10.1016/j.cnsns.2026.109900

11. R. Brociek, A. Wajda, M. Błasik, D. Słota, An application of the homotopy analysis method for the time-or space-fractional heat equation, *Fractal Fract.*, **7** (2023), 224. https://doi.org/10.3390/fractalfract7030224

12. H. Jafari, B. F. Malidareh, V. R. Hosseini, Collocation discrete least squares meshless method for solving nonlinear multi-term time fractional differential equations, *Eng. Anal. Bound. Elem.*, **158** (2024), 107–120. https://doi.org/10.1016/j.enganabound.2023.10.014

13. S. M. Sivalingam, P. Kumar, H. Trinh, V. Govindaraj, A novel L1-predictor–corrector method for the numerical solution of the generalized-Caputo type fractional differential equations, *Math. Comput. Simulat.*, **220** (2024), 462–480. https://doi.org/10.1016/j.matcom.2024.01.017

14. C. P. Li, N. N'Gbo, F. Su, Finite difference methods for nonlinear fractional differential equation with ψ-Caputo derivative, *Physica D*, **460** (2024), 134103. https://doi.org/10.1016/j.physd.2024.134103

15. H. Sun, M. Zheng, Z. Jin, Numerical method for fractional variational problems by Müntz-Legendre polynomials, *J. Comput. Appl. Math.*, **483** (2026), 117390. https://doi.org/10.1016/j.cam.2026.117390

16. M. M. AlBaidani, Numerical solution of fractional third-order nonlinear Emden–Fowler delay differential equations via Chebyshev polynomials, *Axioms*, **15** (2026), 64. https://doi.org/10.3390/axioms15010064

17. W. M. Abd-Elhameed, M. A. Abdelkawy, O. M. Alqubori, A. G. Atta, Pell coefficient polynomials for solving linear hyperbolic first-order partial differential equations via the tau approach, *Electron. Res. Arch.*, **33** (2025), 6012–6035. https://doi.org/10.3934/era.2025267

18. H. S. Osheba, M. A. Ramadan, T. Radwan, An efficient and accurate numerical approach for fractional Bagley–Torvik equations: Hermite polynomials combined with least squares, *Fractal Fract.*, **10** (2026), 37. https://doi.org/10.3390/fractalfract10010037

19. M. H. Heydari, T. Baghban, M. Bayram, M. A. Zaky, Discrete Chebyshev polynomials for two-dimensional fractional optimal control problems involving Caputo-Hadamard derivative, *Int. J. Syst. Sci.*, **57** (2026), 4262–4277. https://doi.org/10.1080/00207721.2025.2600349

20. M. Pourbabaee, Artificial neural networks method based on Gegenbauer polynomials for solving some types of integral equations, *Comp. Appl. Math.*, **45** (2026), 84. https://doi.org/10.1007/s40314-025-03564-6

21. T. T. Zhao, T. J. Wang, J. Tan, Composite spectral collocation method of Legendre-Legendre rational polynomials for the Fokker–Planck equation on unbounded domain, *Math. Comput. Simulat.*, **246** (2026), 188–208. https://doi.org/10.1016/j.matcom.2026.01.035

22. W. A. Khan, S. A. Wani, M. Ayman-Mursaleen, K. Kotecha, P. Jadhav, Extended forms of Legendre-Laguerre-based hybrid polynomials and their characteristics via fractional operator approach, *J. Inequal. Appl.*, **2026** (2026), 24. https://doi.org/10.1186/s13660-026-03437-4

23. U. L. Manikanta, K. J. Gowtham, B. J. Gireesha, P. Venkatesh, A novel Hosoya polynomial collocation approach for evaluating the thermal performance of porous annular fins with internal heat generation employing trihybrid nanofluids, *Int. Commun. Heat Mass*, **172** (2026), 110242. https://doi.org/10.1016/j.icheatmasstransfer.2025.110242

24. N. Samadyar, P. Rahimkhani, Numerical treatment of tumor-immune interaction model of fractional order related to lung cancer via Chelyshkov polynomials, *Math. Methods Appl. Sci.*, **49** (2026), 4056–4073. https://doi.org/10.1002/mma.70333

25. A. AbuGneam, S. Nemati, A. Babaei, Application of generalized fractional-order Bernoulli wavelets in solving distributed-order fractional differential equations, *J. Supercomput.*, **81** (2025), 1348. https://doi.org/10.1007/s11227-025-07760-3

26. H. Hassani, Z. Avazzadeh, A. Turan-Dincel, R. Katani, Application of fractional shifted vieta-fibonacci polynomials in nonlinear reaction diffusion equation with variable order time-space fractional derivative, *Phys. Scr.*, **100** (2025), 025231. https://doi.org/10.1088/1402-4896/adaa38

27. P. Sawangtong, M. Taghipour, A. Najafi, Enhanced numerical solution for time fractional Kuramoto–Sivashinsky dynamics via shifted companion Morgan–Voyce polynomials, *Comp. Appl. Math.*, **44** (2025), 214. https://doi.org/10.1007/s40314-025-03160-8

28. J. Shen, T. Tang, L. L. Wang, *Spectral methods: algorithms, analysis and applications*, Berlin: Springer, 2011. https://doi.org/10.1007/978-3-540-71041-7

29. J. P. Boyd, *Chebyshev and Fourier spectral methods*, 2Eds., New York: Dover Publications, 2001.

30. M. Sahu, P. Roul, S. Khandagale, A B-spline collocation method for a time fractional Black–Scholes model under jump-diffusion, *J. Comput. Appl. Math.*, **487** (2026), 117717. https://doi.org/10.1016/j.cam.2026.117717

31. N. Sarkar, M. Sen, A hybrid Daubechies wavelet collocation approach for a fractional-order SIR epidemic model with delay effects, *Sci. Rep.*, **16** (2026), 2716. https://doi.org/10.1038/s41598-025-32483-z

32. J. Yang, V. Srinivasan, A domain-overlapping algorithm with nonlinear mappings for Chebyshev collocation-based solutions of eigenvalue problems, *Appl. Numer. Math.*, **226** (2026), 87–105. https://doi.org/10.1016/j.apnum.2026.03.012

33. A. A. El-Sayed, S. Boulaaras, F. A. Al-Kharousi, Dickson polynomial-based solutions for fractional order physics problems, *J. Inequal. Appl.*, **2025** (2025), 118. https://doi.org/10.1186/s13660-025-03367-7

34. W. M. Abd-Elhameed, M. A. Abdelkawy, O. M. Alqubori, A. G. Atta, An accurate tau-based spectral algorithm for the time fractional bioheat transfer model, *Bound. Value Probl.*, **2025** (2025), 124. https://doi.org/10.1186/s13661-025-02118-3

35. H. F. Ahmed, W. A. Hashem, A fully spectral tau method for a class of linear and nonlinear variable-order time-fractional partial differential equations in multi-dimensions, *Math. Comput. Simulat.*, **214** (2023), 388–408. https://doi.org/10.1016/j.matcom.2023.07.023

36. C. X. Niu, H. P. Ma, D. Liang, Legendre-tau Chebyshev collocation spectral element method for Maxwell's equations with material interfaces of two dimensional transverse magnetic mode, *Comput. Math. Appl.*, **147** (2023), 222–238. https://doi.org/10.1016/j.camwa.2023.07.024

37. Z. Q. Wang, X. Wen, G. Q. Yao, An efficient spectral-Galerkin method for elliptic equations in 2D complex geometries, *J. Sci. Comput.*, **95** (2023), 89. https://doi.org/10.1007/s10915-023-02207-4

38. S. U. Arifeen, S. Haq, I. Ali, Galerkin approximation of Burgers–Huxley equation with fractional order arising in reaction mechanism and diffusion transport, *Phys. Scr.*, **99** (2024), 125215. https://doi.org/10.1088/1402-4896/ad8b75

39. W. M. Abd-Elhameed, M. A. Abdelkawy, N. M. A. Alsafri, A. G. Atta, Galerkin-based solution for the time-fractional diffusion-wave equation, *Electron. Res. Arch.*, **33** (2025), 5179–5206. https://doi.org/10.3934/era.2025232

40. U. Bayrakci, S. T. Demiray, H. Yildirim, Obtaining new soliton solutions of the fractional generalized perturbed KdV equation, *Phys. Scr.*, **99** (2024), 125202. https://doi.org/10.1088/1402-4896/ad8846

41. H. M. Ahmed, New generalized Jacobi–Galerkin operational matrices of derivatives: an algorithm for solving the time-fractional coupled KdV equations, *Bound. Value Probl.*, **2024** (2024), 144. https://doi.org/10.1186/s13661-024-01948-x

42. K. Sadri, K. Hosseini, E. Hincal, D. Baleanu, S. Salahshour, A pseudo-operational collocation method for variable-order time-space fractional KdV–Burgers–Kuramoto equation, *Math. Method. Appl. Sci.*, **46** (2023), 8759–8778. https://doi.org/10.1002/mma.9015

43. M. Y. Almusawa, H. Almusawa, Numerical analysis of the fractional nonlinear waves of fifth-order KdV and Kawahara equations under Caputo operator, *AIMS Math.*, **9** (2024), 31898–31925. https://doi.org/10.3934/math.20241533

44. C. J. Li, H. X. Zhang, X. H. Yang, A new α-robust nonlinear numerical algorithm for the time fractional nonlinear KdV equation, *Communications in Analysis and Mechanics*, **16** (2024), 147–168. https://doi.org/10.3934/cam.2024007

45. J. Alahmadi, B. Aldossary, E. A. B. Abdel-Salam, Numerical treatment of the coupled fractional mKdV equations based on the Adomian decomposition technique, *Appl. Math. Inform. Sci.*, **18** (2024), 93–99. https://doi.org/10.18576/amis/180110

46. K. Singh, I. Kourakis, Generalized analytical solutions of a Korteweg–de Vries (KdV) equation with arbitrary real coefficients: Association with the plasma-fluid framework and physical interpretation, *Wave Motion*, **132** (2025), 103443. https://doi.org/10.1016/j.wavemoti.2024.103443

47. S. U. Arifeen, S. Haq, Petrov–Galerkin approximation of time-fractional coupled Korteweg–de Vries equation for propagation of long wave in shallow water, *Math. Comput. Simulat.*, **207** (2023), 226–242. https://doi.org/10.1016/j.matcom.2022.12.028

48. S. W. Yao, A. Zafar, A. Urooj, B. Tariq, M. Shakeel, M. Inc, Novel solutions to the coupled KdV equations and the coupled system of variant Boussinesq equations, *Results Phys.*, **45** (2023), 106249. https://doi.org/10.1016/j.rinp.2023.106249

49. M. L. Rupa, K. Aruna, Soliton solutions of time fractional seventh order Korteweg–de Vries equations arises in applied sciences, *Int. J. Appl. Comput. Math.*, **11** (2025), 119. https://doi.org/10.1007/s40819-025-01939-1

50. M. A. Iqbal, M. Hussain, M. Safeer, M. Taj, A. Tounsi, Travelling waves solutions for modified Korteweg-de Vries equation by modified Exp-function method, *Comput. Concrete*, **35** (2025), 155–161. https://doi.org/10.12989/cac.2025.35.2.155

51. A. Alshareef, H. O. Bakodah, Non-central m-point formula in method of lines for solving the Korteweg-de Vries (KdV) equation, *J. Umm Al-Qura Univ. Appl. Sci.*, **11** (2025), 142–152. https://doi.org/10.1007/s43994-024-00154-w

52. Z. A. Noor, I. Talib, T. Abdeljawad, M. A. Alqudah, Numerical study of Caputo fractional-order differential equations by developing new operational matrices of Vieta–Lucas polynomials, *Fractal Fract.*, **6** (2022), 79. https://doi.org/10.3390/fractalfract6020079

53. S. C. Shiralashetti, V. R. Pala, S. I. Hanaji, Bernoulli wavelet integration operational matrix method for the numerical solution of nanofluid flow in an asymmetric porous channel with expanding or contracting wall, *Int. J. Appl. Comput. Math.*, **11** (2025), 155. https://doi.org/10.1007/s40819-025-01978-8

54. H. M. Ahmed, M. Izadi, C. Cattani, A spectral approach to variable-order fractional differential equations: improved operational matrices for fractional Jacobi functions, *Mathematics*, **13** (2025), 2544. https://doi.org/10.3390/math13162544

55. M. O. Enadi, M. A. AL-Jawary, M. Turkyilmazoglu, The operational matrices methods for solving the Poisson equation with nonlocal boundary conditions, *J. Appl. Math. Comput.*, **71** (2025), 2385–2432. https://doi.org/10.1007/s12190-024-02313-y

56. A. Turan-Dincel, S. N. Tural-Polat, Operational matrix method approach for fractional partial differential-equations, *Phys. Scr.*, **99** (2024), 125254. https://doi.org/10.1088/1402-4896/ad8f7a

57. R. V. Shree, B. P. Mallikarjun, B. Souayeh, S. Bhattacharya, Application of Fibonacci wavelet frame operational matrix for the analysis of Arrhenius-controlled heat transfer flow in a microchannel, *Case Stud. Therm. Eng.*, **63** (2024), 105326. https://doi.org/10.1016/j.csite.2024.105326

58. M. A. Abdelkawy, W. M. Abd-Elhameed, S. S. Alzahrani, A. G. Atta, A. Biswas, Numerical solutions via shifted Pell polynomials for third-order Rosenau–Hyman and Gilson–Pickering equations, *Mathematics*, **14** (2026), 582. https://doi.org/10.3390/math14030582

59. O. M. Alqubori, S. A. Alsulami, A. G. Atta, A. K. Amin, W. M. Abd-Elhameed, Numerical scheme for solving the time-fractional Huxley equation using shifted Dickson polynomials, *AIMS Math.*, **11** (2026), 13744–13766. https://doi.org/10.3934/math.2026566

60. W. M. Abd-Elhameed, A. H. Al-Mehmadi, N. M. A. Alsafri, O. M. Alqubori, M. Adel, A. G. Atta, Spectral collocation approach for solving the time-fractional Kuramoto–Sivashinsky equation using the Fibonacci coefficient polynomials, *AIMS Math.*, **10** (2025), 18070–18093. https://doi.org/10.3934/math.2025805

61. S. Kumar, V. Gupta, D. Zeidan, An efficient collocation technique based on operational matrix of fractional-order Lagrange polynomials for solving the space-time fractional-order partial differential equations, *Appl. Numer. Math.*, **204** (2024), 249–264. https://doi.org/10.1016/j.apnum.2024.06.014

62. M. Kashif, M. Singh, T. Som, E. M. Craciun, Numerical study of variable order model arising in chemical processes using operational matrix and collocation method, *J. Comput. Sci.*, **80** (2024), 102339. https://doi.org/10.1016/j.jocs.2024.102339

63. I. Podlubny, *Fractional differential equations: An introduction to fractional derivatives, fractional differential equations, to methods of their solution and some of their applications*, New York: Academic Press, 1998.

64. S. Saleem, M. Z. Hussain, Numerical solution of nonlinear fifth-order KdV-type partial differential equations via Haar wavelet, *Int. J. Appl. Comput. Math.*, **6** (2020), 164. https://doi.org/10.1007/s40819-020-00907-1

65. H. O. Bakodah, Modified Adomian decomposition method for the generalized fifth order KdV equations, *Am. J. Comput. Math.*, **3** (2013), 53–58. https://doi.org/10.4236/ajcm.2013.31008

66. W. M. Abd-Elhameed, H. M. Alshehri, M. H. Alharbi, O. M. Alqubori, A. K. Amin, A. G. Atta, Shifted Pell–Lucas polynomial-based algorithms for fractional and classical Rosenau–Hyman models, *Fractal Fract.*, **10** (2026), 359. https://doi.org/10.3390/fractalfract10060359

67. W. M. Abd-Elhameed, O. M. Alqubori, A. G. Atta, A collocation approach for the nonlinear fifth-order KdV equations using certain shifted Horadam polynomials, *Mathematics*, **13** (2025), 300. https://doi.org/10.3390/math13020300